NILU
TEKNISK NOTAT NR 12/75
REF:
DATE: OCTOBER 1975

DESIGN AND CONSTRUCTION OF NILU'S PIEZOELECTRIC MASS MONITOR (PPM)

Dr. A. Richard Stiles
Project Consultant

Dr. David L. Brenchley
NTNF Research Fellow

A Report Submitted to
Norwegian Institute for Air Research

Kjeller, Norway
11th March 1975

NORWEGIAN INSTITUTE FOR AIR RESEARCH
P. O. BOX 115, 2007 KJELLER
NORWAY

Table of Contents

Chapter 1

INTRODUCTION

In March 1974 NILU's instrument laboratory personell (Messrs. Berg and Larssen) indicated an interest in having a piezo-electric mass monitor (PMM) for measuring atmospheric aerosol concentrations. Such an instrument was needed to increase the aerosol monitoring capability for aircraft measurement programs. It was decided that Dr. David L Brenchley and Dr. A Richard Stiles should work together to design and build such an instrument. Thus as shown in Figure 1-1, Dr. Stiles agreed to be a consultant and the project was started. After the construction stage further plans would then be made at NILU for performance tests, calibration and field testing the instrument. Drs. Stiles and Brenchley also agreed to prepare this report on piezoelectricity and the specific details on the NILU PMM instrument.

The construction was completed by Dr. Stiles in September 1974, and the instrument was shipped to NILU in October. Since this time the instrument has been inspected and bench operated but no specific set of performance tests have been performed. This stage of the work has been partly delayed because NILU does not have adequate aerosol generation equipment. However, in February 1975 such equipment was ordered, and it should be available for use by May or June 1975. Then, more extensive testing of the PMM can be carried out. It is intended that evantually this instrument will be used in projects studying the long range transport of air pollutants.

Kjeller, 5th April, 1974

AGREEMENT

This agreement, between Dr. A. Richard Stiles, 1128½ North 7th, Lafayette, Indiana 47901, USA, and Norwegian Institute for Air Research, Postboks 115, 2007 Kjeller, Norway, concerns co-operation on building and use of one piezoelectric mass monitor (PMM) according to the following text :

1. Dr. Stiles shall (1) design and construct the PMM electronics and EP systems, (2) supply detailed circuit diagrams and parts lists for use in trouble shooting and construction of other units, (3) supply a brief write-up describing the features of the system, (4) correspond with Dr. Brenchley and others at NILU to adequately interface the mechanical and electrical systems.

2. NILU will (1) acknowledge Dr. Stiles as a project consultant to NILU, (2) supply funds for purchase of all components for the electical system, (3) design and construct the collector head assembly and ship it to Dr. Stiles, (4) list Dr. Stiles as an author of any technical papers or publications pertaining to the PMM and acknowledge Dr. Stiles' work in any projects using the PMM.

3. The instrument is expected to be finished by September 1974. Both parties are responsible for this time limit and must discuss the dependancy of each other.

4. The final payment from NILU for the components is to be based on receipts. However, NILU shall forward $ 200. The estimated total cost of maximum $ 500 must not be exceeded without notice in order to discuss whether to continue or not with the project.

5. Both parties must make sure that they satisfy customs regulations etc. when sending any parts of the equipment to each other. (For instance must invoices, pro forma or real, be available by reception.)

Dr. A. R. Stiles

Dr. B. Ottar, Director

P. Berg, Business Manager

Norwegian Institute for Air Research

Figure 1-1 Statement of Agreement

Chapter 2

LITERATURE REVIEW

The piezoelectric microbalance has been used to effectively measure the thickness of vacuum-deposited metal films (1). Recently the method has been applied to monitoring of ambient aerosols (2). Brenchley and Carpenter (3) have reviewed the method and discussed its application to source monitoring.

Principle of Operation

When certain types of crystals are put under a mechanical stress they respond by having electical charges appear on certain faces of the crystal. Conversely a mechanical stress results when the crystal is subjected to external electical fields at the crystal surface. This phenomenon is called piezoelectricity. It has been understood for many years and one of the best known applications is the quartz pressure transducer (4).

The piezoelectric effect for mass measurements is useful when the crystal is made a part of an electrical oscillator circuit. The crystal will vibrate mechanically when placed in the oscillating electrical field. If the electric field oscillates at a frequency close to the mechanical resonant vibration frequency of the crystal forces the circuit to oscillate at precisely the resonant frequency. It is this important effect which allows the piezoelectric crystal to be used as a mass monitor. When a small quantity of foreign material is deposited on the surface of a crystal, the natural resonant frequency of the crystal decreases. The frequency of vibration is expressed

$$f = \frac{N}{L} \qquad (2\text{-}1)$$

where

f is the frequency of vibration
N is the constant for fundamental mode
L is characteristic dimension for vibration

Thus the characteristic dimension for vibration is the crystal thickness and it is this parameter which is changed when a layer of particulate matter is deposited on the surface. Since frequency can be measured so precisely, the resulting decrease in resonant frequency of the crystal allows a corresponding precise mass measurement.

The fact that an oscillating quartz crystal may be used to detect a change in mass has been known almost as long as quartz crystal oscillators have been in use. For example, in early radio days it was common practice to lower the transmitter frequency by marking the surface of the controlling quartz plate with a pencil, thus adding an adhering mass of graphite (1).

Thin Film Theory

The application of the piezoelectric microbalance stems from the consideration of the deposited foreign material as a thin film. The theory was originally presented by Sauerbrey (5) in conjuction with metal film evaporation and later confirmed by Olin and Sem (2) for particle deposition on a crystal. Figure 2-1 shows a side-view of a crystal with particulate matter attached.

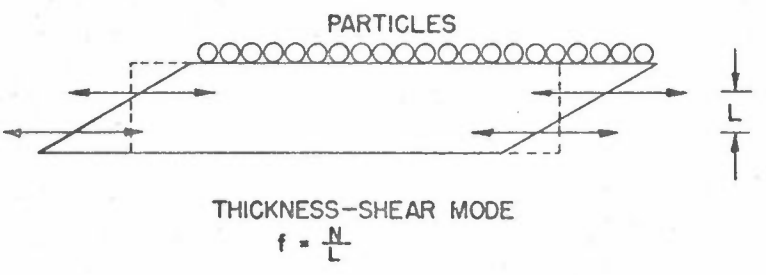

Figure 2-1 : Piezoelectric crystal.

The thickness of a crystal may be expressed as

$$L = \frac{M_q}{A \rho_q} \qquad (2\text{-}2)$$

where

M_q is the mass of the electrically driven portion of the crystal

A is the area of the electrically driven portion of the crystal , and

ρ_q is the mass density of the crystal.

Differentiating Equation 2-1, we obtain

$$\frac{\Delta f}{f} = - \frac{\Delta L}{L} \qquad (2\text{-}3)$$

where Δf is the change in resonant frequency caused by a change in the thickness ΔL of the crystal. Differentiating Equation 2-2 and substituting into Equation 2-3 we obtain

$$\frac{\Delta f}{f} = \frac{\Delta M_q}{\rho_q A L} = - \frac{\Delta M_q}{M_q} \qquad (2\text{-}4)$$

At this point an assumption is made that the frequency shift caused by the change in mass, ΔM_q, will also be caused by an identical foreign mass, ΔM, deposited on the surface. This then also implies that the foreign particles strictly adhere to the crystal surface. This necessarily means that the layer must be very thin.

Under the thin film condition the foreign material has a negligible contribution to the elastic properties of the crystal. For thick layers a composite resonator exists and the collected material is also strained and the thin film theory no longer applies. When this occurs the observed frequency change will be less than that predicted by thin film theory. In general, a layer will act as a thin film if the deposited layer is less than 1% of the crystal thickness (2). The assumptions of thin film theory allow Equation 2-4 to become

$$\frac{\Delta f}{f_o} = - \frac{\Delta M}{M_{q_o}} \qquad (2\text{-}5)$$

where subscript "o" refers to the initial condition before any foreign mass is added. This equation indicates that the resonant frequency decreases linearly with the addition of foreign mass. In practice it has been found that the deviation from linearity is less than 1% as long as Δf is less than 1/2% of f_o. Substituting Equation 2-1 into Equation 2-5 and rearranging we obtain

$$\frac{\Delta f}{\Delta M} = -\frac{C_f}{A} \qquad (2\text{-}6)$$

where C_f is a constant for a specific type crystal and is defined

$$C_f = \frac{f_o^2}{\rho_q N} \qquad (2\text{-}7)$$

Equations 2-6 and 2-7 indicate that crystals which have higher resonant frequencies, f_o, will have correspondingly higher mass sensitivities. However, as will be discussed later, there is an upper limit to this because at higher frequencies particle reentrainment becomes more of a problem.

Material Requirements

The piezoelectric crystals must possess several important characteristics in order to be successfully used as part of a microbalance. These are mechanical and chemical in nature. First, the crystal must have a low internal friction, and second, the material must be essentially inert to its environment. This latter factor is critical because a surface chemical reaction of the crystal could cause its weight to increase or decrease. It would be impossible to separate this weight change from that collected on the surface.

With the foregoing consideration in mind, quartz is a material which best meets these requirements. Also, it has a very high frequency stability, i.e. 1 part in 10^9. Thus at present all piezoelectric microbalances use some sort of quartz crystal. The properties of the crystal vary somewhat depending on how it is cut. The AT-cut crystal finds the greatest use in aerosol monitoring because it is a high

frequency cut possessing a low temperature coefficient. This latter property is desirable if frequency change is to occur as a function of collected mass. When the material properties associated with the AT-cut quartz crystal are applied to Equation 2-7, we obtain

$$C_f = 2.27 f_o^2 \qquad (2\text{-}8)$$

ρ_q is 2.654 g cm^-

N is 0.166 MH_z - cm, and thus,

C_f is in $\frac{H_z - cm^2}{\mu g}$ and

f_o is in MH_z

Components

The basic components of a piezoelectric microbalance aerosol detector are the collection method, the crystal and the detection electronics. The aerosol must be collected or deposited efficiently on the crystal surface. The crystals should have the properties previously discussed and the electronic detection system is composed of the oscillation circuits, a mixer, and a read-out apparatus for the frequency. The approach is to optimize the unit by designing for the most efficient removal mechanism, selecting a crystal with a sufficiently high mass sensitivity and then operating the device so that the frequency change caused by all other factors is negligible compared to that caused by the collected mass.

Crystal Characteristics

The quarts crystals take the shape of flat plates or circular wafers. They are quite small and have an electrode on

each side. The electrodes are gold, silver, nickel or aluminum and are deposited by vacuum evaporation techniques. Only that portion of the crystal which is covered by the electrode is sensitive to collected mass. This is true because the amplitude of vibration dampens very rapidly outside the electrode area. The crystal becomes a part of the electrical circuit by attaching leads or clips to each side. While in operation the results of the mass measurements are not affected by normal mechanical shock or vibration. In addition, the crystal will function equally well in any mounted position.

Particle Collection

The aerosol may be deposited upon the crystal surface by the following mechanisms : inertial impaction, electrostatic precipitation, thermal precipitation, centrifugal separation and gravity. Of these, the first two mechanisms are most commonly used. Figure 2-3 shows the side-view of devices used to collect the aerosol. In one case the sample stream enters through a jet and the particles impinge on the crystal surface. In the other device the crystal is actually the collecting electrode of an electrostatic precipitator. The needle valve is the discharge electrode and is located in the incoming gas stream. The particles thus become charged and are attracted to the crystal surface. The important point here is that either the aerosol should be completely collected or the exact collection efficiency of the device must be known. In most cases it is necessary to know the collection efficiency as a function of particle size.

Particle Adhesion

Once the particle has been effectively removed from the gas stream it remains on the surface due to adhesion forces.

Inertial forces tend to reentrain the particle because of crystal vibration. These forces are represented as follows (5)

$$F_a \alpha D_p \qquad (2\text{-}9)$$

$$F_i \alpha D_p^3 \; f_o^2 \qquad (2\text{-}10)$$

where

F_a is the force causing the particle to adhere to the crystal surface

F_i is the force tending to reentrain the particle

D_p is the particle diameter

f_o is the resonent frequency of the crystal.

Equations 2-9 and 2-10 indicate that the larger particles will tend to be reentrained, but this can be alleviated somewhat by using crystals with lower resonant frequencies, f_o. However, as indicated in Equations 2-6 and 2-7 this will result in a lower mass sensitivity of the system.

The particle collection and containment process can be enchanged by conditioning the aerosol and/or altering the crystal surface. Certain gas phase constituents such as water vapor, ammonia and sulfur dioxide, can be used to enchange the particle collection and adhesion characgeristics. Also a thin coating of adhesive material such as grease can be applied to the crystal. These methods may help to decrease particle reentrainment but they raise other uncertainties which must be considered. Care must be taken not to overload the crystal with the coating and cause it to be in a non-linear response regime. Also, the gas conditioning agents which are added are undoubtedly adsorbed onto the aerosol and will therefore be measured along with the collected aerosol. The coating put onto the crystal may also off-gas

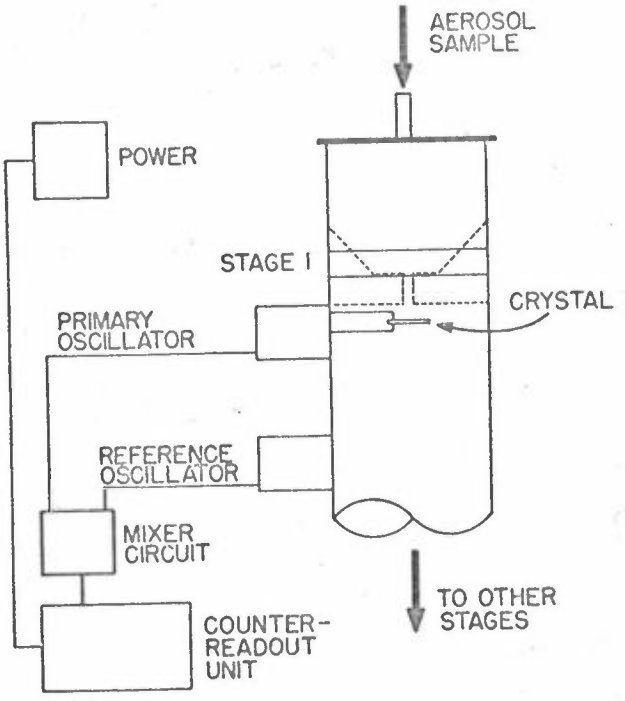

(a) Cascade impactor

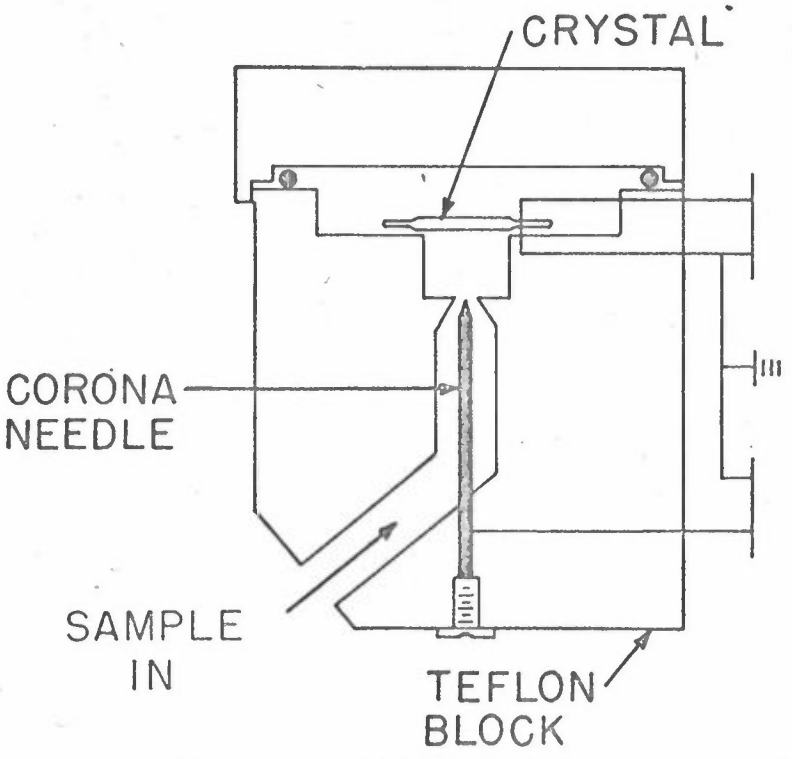

(b) Electrostatic precipitator

Figure 2-2. Devices for Collecting Aerosols on Piezoelectric Crystals (3,6)

or adsorb gases which may then cause error. These problems can only be handled by using careful calibration procedures.

The piezoelectric crystals must have their surfaces cleaned periodically. This requirement stems from the thin film theory and the possibility of deviating from linearity. The crystals otherwise simply become overloaded. The cleaning is accomplished by using a piece of tissue paper possibly in conjunction with a washing solution. It is not necessary to clean it up so that the original resonant frequency is obtained. Mass measurement is based upon frequency change and thus it is acceptable if some residual mass is still present.

Electronic System

The piezoelectric microbalance may consist of one or two crystals. If one crystal is used, a high frequency counter capability is a necessity. The resonant frequencies of the clean crystals are usually $5MH_Z$ or 10 MH_Z and require high frequency counters. This problem can be avoided if two crystals are used. One crystal is used as a reference, while the second collects the aerosol material. The outputs of these two oscillator circuits are fed into a mixer basically subtracts the two signals. The frequency difference is then read as the output. Hopefully the reference crystal accounts for any changes in frequency due to environmental factors other than added mass. Details of the various electronic circuits will not be presented here.

Operating Conditions

The operating conditions of a microbalance must be known and held constant. As mentioned previously the crystals are sensitve to temperature. This variable can be controlled by proper selection of crystal cut and maintaining conditions to keep the temperature coefficient low. For example, the

AT-cut quartz crystal exhibits a frequency deviation of less than 0.001% in the 20°C to 60°C range. This change is therefore negligible compared to that caused by the addition of the micrograms of material.

Some care must also be taken with regard to pressure. The gas pressure may affect crystal response due to stressing and gas adsorption - desorption processes. Olin and Sem (7) performed tests and indicated a 12 Hz change for a static pressure change of 25 cm of Hg. This should not be a serious source of error but it should be considered. Frequency readings should be made at the same pressure if possible.

Aerosol Concentration

The concentration, C, of an aerosol in a gas stream can be calculated from the following expression :

$$C = \frac{\Delta f}{\Delta t} \frac{1}{S\ Q\ E_c\ E_w} \qquad (2\text{-}11)$$

where

- C is the concentration in $\mu g\ m^{-3}$
- Δf is the change in frequency, Hz
- Δt is the sampling time, sec.
- Q is the sample flow rate, $m^3\ sec^{-1}$
- S is the theoretical mass sensitivity of the crystal, Hz μg^{-1} (from Equation 2-6)
- E_c is the efficiency of particle collection by the collector
- E_w is the efficiency of the piezoelectric microbalance in weighing the deposited particles.

In this expression Δf, Δt, and Q are quite easily measured. The theoretical mass sensitivity is calculated based upon the known characteristics of the crystal. The efficiencies, E_c and E_w, are not known usually, without performing calibration tests. The collection efficiency for a given device

may be estimated from theory based upon design and operating conditions. The electrostatic precipitator technique will usually have a higher collection efficiency than inertial impactor techniques. The E_w term will most likely be close to a value of 1.0 if the thin film theory conditions are met. It should be pointed out there that both E_c and E_w are dependent upon the particle size.

Particle Sizing

The piezoelectric microbalance has some capability for determining aerosol size distributions. There are two approaches available. One is the method of Carpenter (6) in which several crystals were used in conjunction with a multiple stage cascade impactor that separated the aerosol into various size ranges. In the second approach the sampled gas must be diluted so that no two particles are collected at the same instant. Thus a change of frequency over a short period of time can be attributed to a single particle, and if it is assumed to be spherical with a constant and known density its size can be calculated. All of this can be automatic if the digital output of the frequency counter is converted to analog and then differentiated. Additional electronics must be used to count the number of frequencies associated with each size category. For a material with a density of 2 g cm^{-3}, particles as small as 0.5 microns can be detected.

Calibration

If the design and operation of the microbalance meets the theoretical assumptions, no calibration is necessary. The response is linear and predictable. If the layer becomes thick and/or the collected material is dissipative, the method can still be used, but a laboratory calibration is necessary. This means that the method can actually be extended to the detection of liquids and gases, but calibration is then a necessity.

Equipment

There have been a number of piezoelectric mass monitors constructed, some of which are available commercially. Most of them have been designed for a specific application.

Thermo-Systems, Inc., of St. Paul, Minnesota, has developed a line of instruments designed for monitoring aerosol concentrations under ambient conditions and from emission sources. These instruments are single stage collectors using the electrostatic precipitator design (see Figure 2-2). The precipitator operates at 5000 vdc. The 5 MHz quartz crystals are housed in a Teflon chamber and have a mass sensitivity of 180 Hz μg^{-1}. A monitoring and a reference crystal are used. The sample flow rate through the instrument is 1 LPM. Applying this data and assuming E_c and E_w to be unity to Equation 2-11, we obtain the manufacturer's expression for aerosol concentration

$$C = 333 \frac{\Delta f}{\Delta t} \qquad (2\text{-}12)$$

The particle mass monitors are designed to collect particles in the 0.01 to 20 micron range. The maximum amount of material which can be collected before the crystal must be leaned is 40 micrograms. This restraint in conjunction with the 1 LMP sample flow rate means that the crystals must be cleaned every several hours under high concentration conditions. Of course, the very low concentrations would allow the crystals to be used a couple days before cleaning.

Celesco Industries of Costa Mesa, California, has developed a single state impactor which uses 10 MHz crystals and has a mass sensitivity of 1000 Hz μg^{-1} (8). A two crystal circuit is used with the second one being a reference crystal. The collection efficiency of the monitoring crystal is increased by placing a thin 10^{-4} cm layer of adhesive on the

surface. The instrument is designed to collect particles in the 0.1 to 100 micron size range and can be used for aerosol concentrations of 10 $\mu g\ m^{-3}$. The sample flow rate used is 0.15 LPM. Recently Celesco has used this method and built a multiple stage cascade impactor.

Carpenter (6) fabricated a four stage cascade impactor after the design of Mitchell and Pilcher (9) and equipped each stage with 10 MHz crystals. A dual crystal oscillator circuit was employed with one reference crystal and a monitoring crystal located at each stage. A single mixer and digital read-out unit was used. A switch was used to monitor each stage separately. The impactor operated at a flow rate of 0.5 LMP and for an aerosol with density of 1 $\mu g\ cm^{-3}$ had stage constants of 18.9, 12.6, 6.3, and 2.5 microns respectively for the four stages. The unit was calibrated using a uranine dye aerosol which was analyzed by a simple fluorescence analysis using a spectrophotometer. Figure 2-3 shows the results of the calibration tests for the jet which had a stage constant of 6.3 microns. Note that the calibration line agrees quite well with the calculated theoretical mass sensitivity of 923 Hz μg^{-3}. This was not the case for the other stages, however, as particle deposition became a problem. At the top two stages, particles were collected over an area greater than that covered by the electrodes, thus causing the observed mass sensitivity to be lower than theoretical. On the fourth stage the aerosol was not being uniformly distributed over the crystal surface. Although still in a linear response regime, the observed mass sensitivity was greater than theoretical. This situation is explained by reexamining Equation 2-6 and realizing that "A" was effectively being decreased due to the smaller jets at the lower stages. In stage 3 the jet size and the electrode area were essentially the same. All this does not pose a problem as long as the unit is properly calibrated.

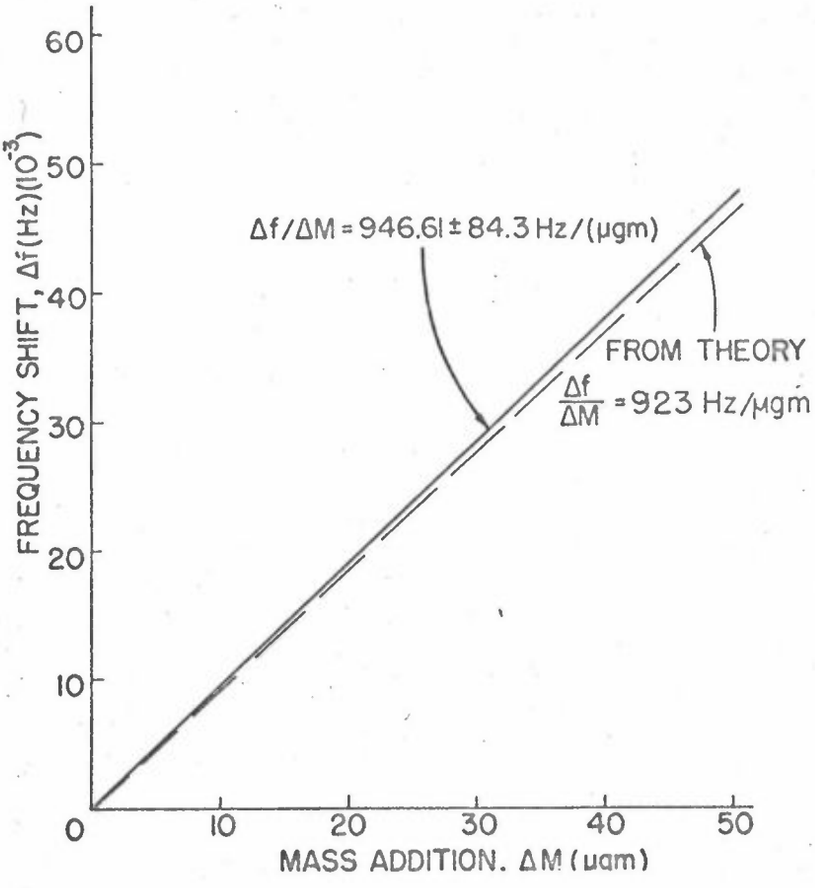

Figure 2-3. Calibration Curve for Piezoelectric Mass Monitor (3)

Applications

The piezoelectric microbalance has found applications for aerosol monitoring in ambient air and various sources. These applications have met with varying degrees of success. Table 2-1 shows the advantages and disadvantages of piezoelectric method.

Both the Thermo-Systems and Celesco units have been successfully used to monitor aerosols in the ambient air (10, 11). Thermo-Systems (12) reports a good correlation of the piezoelectric device with a filtration method. Chuan (10) reports that ambient aerosol concentrations were successfully measured with an airborne instrument; in a test in Los Angeles, concentrations ranged from 197 $\mu g\ m^{-3}$ in the wake of a jet aircraft taking off to 2 $\mu g\ m^{-3}$ at an altitude of 5000 feet.

The microbalance instruments have been applied to source testing of automobiles and powerplants with some success. The major problems in this type of application are the high aerosol concentrations and the presence of interfering substances such as water vapor. Herling (13) has reported tests on automobile exhaust and indicated a ± 30% deviation from filtration measurements. Herling attributes this variation to the presence of organics and water vapor. Sem (14) has outlined a method for using the piezoelectric crystal to monitor particulate matter from power plant stacks.

This system is shown in Figure 2-4. Notice that the isokinetic sampling process must be done twice. First, the sampling rate from the stack must be sufficient to provide an adequate sample. Second, the sample must be split because the particle mass monitor can accommodate only a small flow rate. The sample conditioning, which usually consists of heating or dilution, is needed to prevent condensation on the piezoelectric crystal.

Advantages

1. Very high mass sensitivity
2. Linear response
3. Light weight and portable
4. Fast response
5. Response unaffected by shock and vibration
6. Moderate cost
7. Can provide total mass or size distribution data

Disadvantages

1. Crystals are not cleaned automatically and hence requires attention
2. Particle reentrainment may be a problem
3. Volatile components are lost
4. Condensation may be a problem
5. Temperature limitations
6. Difficulty getting even particle distribution on crystals
7. Response may be affected by gaseous constituents also

Table 2-1: The Advantages and Disadvantages of the Piezoelectric Method

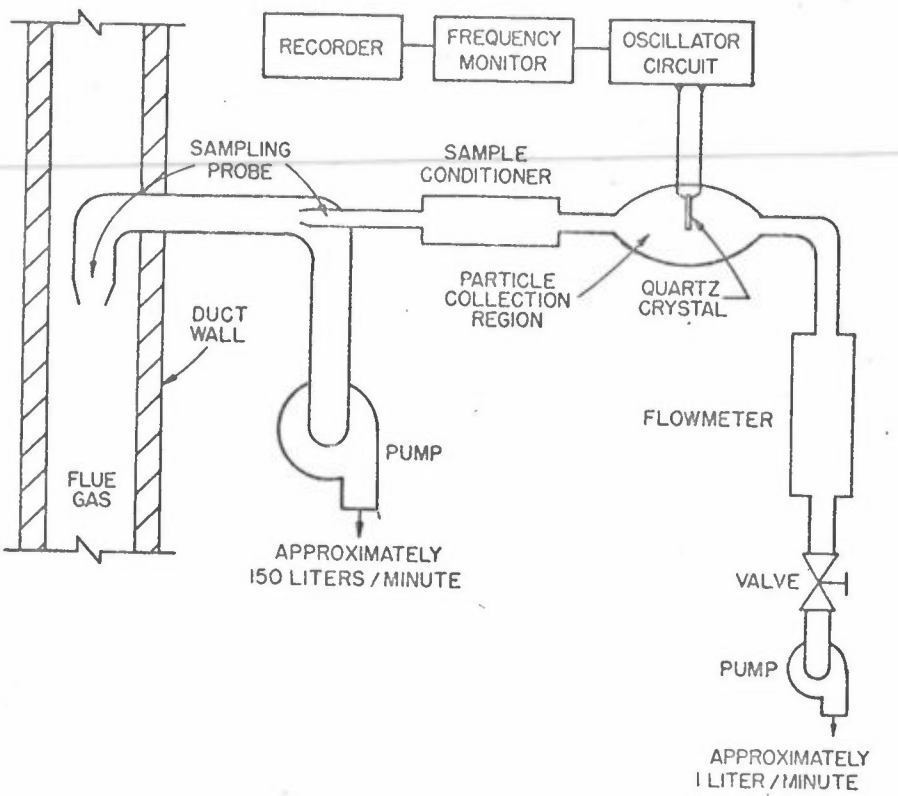

Figure 2-4: Source sampling scheme using Piezoelectric Mass Monitor

Summary

The piezoelectric microbalance shows promise for many types of applications for aerosol monitoring. It is particularly effective for work conditions where the temperature and water vapor problem is negligible. The application for monitoring source concentrations of aerosols seems presently open to question. The eventual success of such an application hinges on the characteristics of the gas stream and the aerosol. The final evaluation of this method for a particular application stems from a consideration of the advantages and

disadvantages. Basically the application of the piezo-electric microbalance for aerosol monitoring is in its infancy and many of its present problems will probalby be worked out in the future.

REFERENCES

1. Wolsky, S. P. and Danuk, E. J. Z. (editor). Ultra Micro Weight Determination in Controlled Environments, Interscience Publishers, New York, New York, 1969.

2. Olin, J. G. and Sem, G. J. "Piezoelectric Microbalance for Monitoring the Mass Concentration of Suspended Particles," Atmospheric Environment 5:653 (1971).

3. Brenchley, D. L. and Carpenter, T. E. "Monitoring Aerosol Concentrations with Piezoelectric Crystals," Proceedings of the 12th AEC Air Cleaning Conference, Oak Ridge, Tenn., October, 1972.

4. Beckwith, T. G. and Buck, N. L. Mechanical Measurements. Addison-Wesley Publishing Co., Reading, Massachusetts. 1961.

5. Sauerbrey, G. Z. "Verwendung von Schwinquarzen zur Wagung dunner Schichten und zur Mickro-wagung." Ziets. Phys. 155, 206 (1959).

6. Carpenter, T. E. "The Design, Construction and Calibration of a Piezoelectric-Cascade Impactor for Monitoring Aerosols," M. S. Thesis, School of Civil Engineering Purdue University, 1972.

7. Olin, J. G. and Sem, G. J. "Piezoelectric Aerosol Mass Concentration Monitoring," Advances in Instrumentation for Air Pollution Control, Symposium, Cincinnati, Ohio, May, 1969.

8. Chuan, Raymond L. "An Instrument for the Direct Measurement of Particulate Mass," Aerosol Science, Vol. I, 111 (1970).

9. Mitchell, R. I. and Pilcher, J. M. "Improved Cascade Impactor for Measuring Aerosol Particle Size," Ind. and Eng. Chem., 51, 1039 (1959).

10. Chuan, R. L. "Measurement of Particulate Pollutants in the Atmosphere." AIAA Paper No. 71-1100, Joint Conference on Sensing of Environmental Pollutants, Palo Alto, California, 1971.

11. Olin, J. G. "Airborne Particle Monitoring Applications of the Particle Mass Monitor System," AIAA Paper No. 71-1100, Joint Conference on Sensing of Environmental Pollutants, Palo Alto, California, 1971.

12. "Air Quality Monitoring Experiments with Particle Mass Monitor System," Technical Note No. 6, Thermo-System Inc., St. Paul, Minnesota.

13. Herling, R. "A Comparison of Automotive Particle Mass Emission Measurement Techniques," Central States Meeting of the Combustion Institute, Ann Arbor, Michigan.

14. Sem, G. J., Porgos, J. A., and Olin, J. G. "Monitoring Particulate Emissions," Chem. Engr. Prog. Vol. 67, No. 10 (1971).

ADDITIONAL REFERENCES

Sauerbrey, G.Z., "Measurements of the Amplitude Distribution of Vibrating AT-cut Crystals by Means of Optical Observations." Proceedings, 17th Annual Frequency Control Symposium, Army Electronics Research and Development Laboratory, Ft. Monmouth, N.J., 1963.

Pulker, H.K. and W. Schadler, "Factors Influencing the Accuracy of a Quartz Crystal as a Thickness Monitor for Thin-Film Deposition," Il Nuovo Cimento, 57B:19-24 (1968).

Guilbault, G. G., and Lopez-Poman, A., "Use of Piezoelectric Crystals as Sensitive and Specific Detectors for SO_2," Analytical Letters, 5 (4), 225 (May 1972)

King, W. H., Jr., "Piezoelectric System Detector," Analytical Chemistry, Vol. 36, No. 9,(August 1964)

Olin, J.G., G.J. Sem and D.L. Christenson, "Piezoelectric-Electrostatic Aerosol Mass Concentration Monitor," Am. Ind. Hyg. Assoc. J., 32:209-220 (1970).

Olin, J.G., R.P. Trautner, and G.J. Sem, "Air-Quality Monitoring of Particle Mass Concentration with a Piezoelectric Particle Microbalance," Paper No 71-1, 64th Annual Meeting, Air Pollution Control Association (June 27 - July 1, 1971).

Olin, J.G., "Design and Operation of a Piezoelectric/Electrostatic Particle Microbalance for Automatic Monitoring of the Mass Concentrations of Air-Borne Particles," Paper 71-558, Instrument Society of America, International Conference and Exhibit, Chicago, Ill., Oct. 4-7, 1971.

Chuan, R.L., "Measurement of Particulate Pollutants in the Atmosphere," Joint Conference on Sensing of Environmental Pollutants, (Sponsored by Am. Inst. of Aeronautics and Astronautics, et al.) Palo Alto, Calif., Nov. 8-10, 1971.

State of the Art: 1971, Instrumentation for Measurement of Particulate Emissions from Combustion Sources. National Technical Information Service (Report PB 202 666) Springfield, VA 22151 (1971).

Frechette, M. W. and Fasching, J. L., "Simple Piezoelectric Probe for Detection and Measurement of SO_2" Environmental Science & Technology 7:13, 1135-1137 (December 1973)

Chapter 3

INSTRUMENT DESIGN

Performance Requirements

A piezoelectric mass monitor (PMM) was needed by NILU. The Long Range Transport study required instruments to monitor aerosols by using an instrumented aircraft. In this respect the performance requirements for a PMM instrument were defined. The instrument should:

-- be portable and of a size suitable for mounting in an aircraft.

-- operate on a 12 vdc negative power supply.

-- have a low power use.

-- be able to collect and monitor aerosols in the 0.1 to 10 micron size range.

-- be able to provide a continuous measurement of aerosol concentration.

-- be able to detect a minimum concentration of one microgram per cubic meter.

-- provide both a digital output and signal for tape system.

-- have the capability to vary the length of sampling time period and the sampling interval period.

-- be able to clean or change the crystals during use in the field.

Instrument Characteristics

The following decisions were made about the instrument's characteristics.

-- The particles would be collected with an electrostatic precipitator. It was felt that an impactor system would not have adequate collection efficiencies for the very small particles.

-- Solid state components would be used wherever possible. This would decrease the size and weight while at the same time increase the reliability.

-- An air pump would not be included in the instrument. The venturi system on the aircraft could be used and critical flow conditions could be used to maintain constant air flow rates.

-- The sample pretreatment system, if needed, would not be put on the instrument until it had been tested in the laboratory and tried on an aircraft.

-- The sampling head would be made of Teflon. This material has excellent thermal, chemical and electrical properties.

-- The instrument would have different operation modes inorder to reduce power use. For example the LED output need not be in continuous operation.

-- There should be a warning system so that the instrument would not be operated with overloaded crystals. Without such a system it would be easy to make erroneous measurements and not know about it.

Instrument Layout

Figure 3-1 shows the general layout chosen for the PMM. All components are mounted in a standard-type instrument case. Circuit boards are used throughout. Details on the electrical system are given in Chapter 4.

The details for the sampling head are shown in Figure 3-2. The sample is drawn into the sampling head by a vacuum such as a pump or venturi. No flow control valve or orifice are shown but these must be used. The sample flows into the Teflon from the back. It flows around a needle which acts as a discharge electrode and charges the aerosol. The surface of the first crystal is the collecting electrode. A secondary collecting electrode is used to capture any particles carried over from the primary collection electrode. The sample then flows through the Teflon block to the second crystal. This is the reference crystal and it is used to compensate for temperature and humidity. The sample then passes out of the Teflon head and into the instrument case.

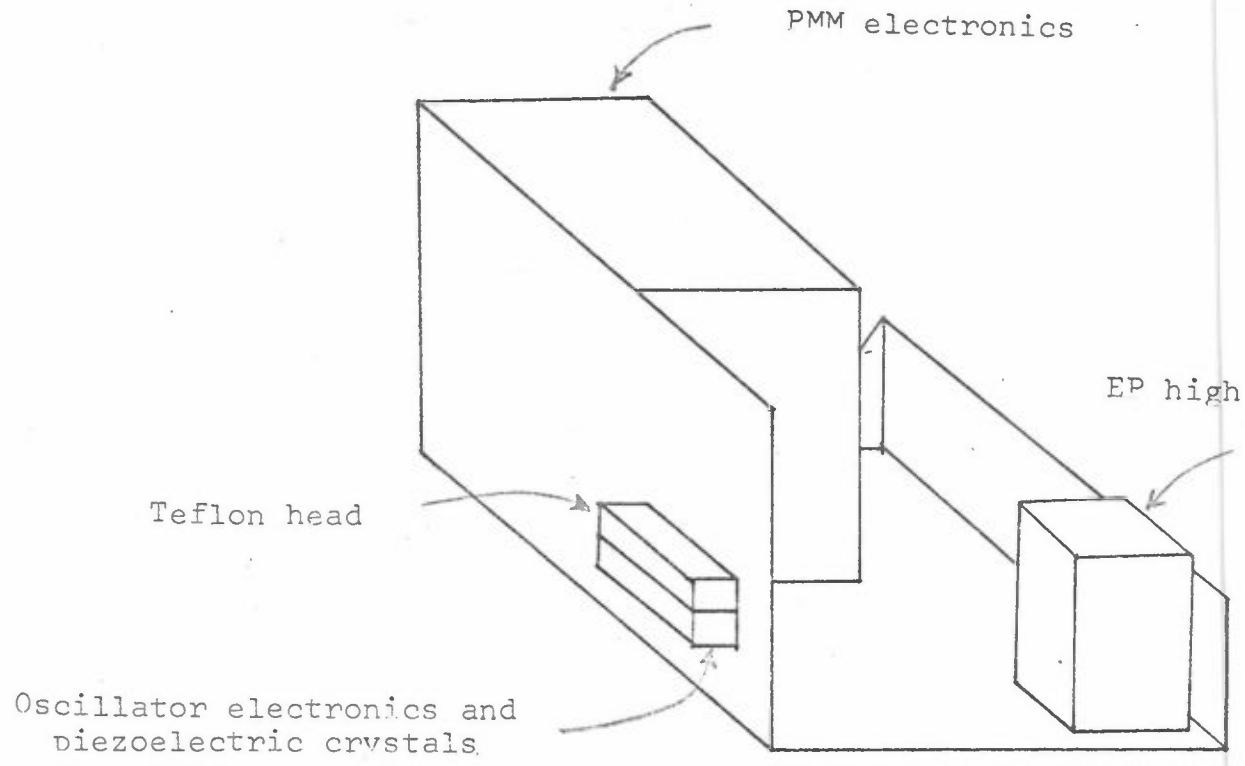

Figure 3-1. Schematic Layout of NILU PMM

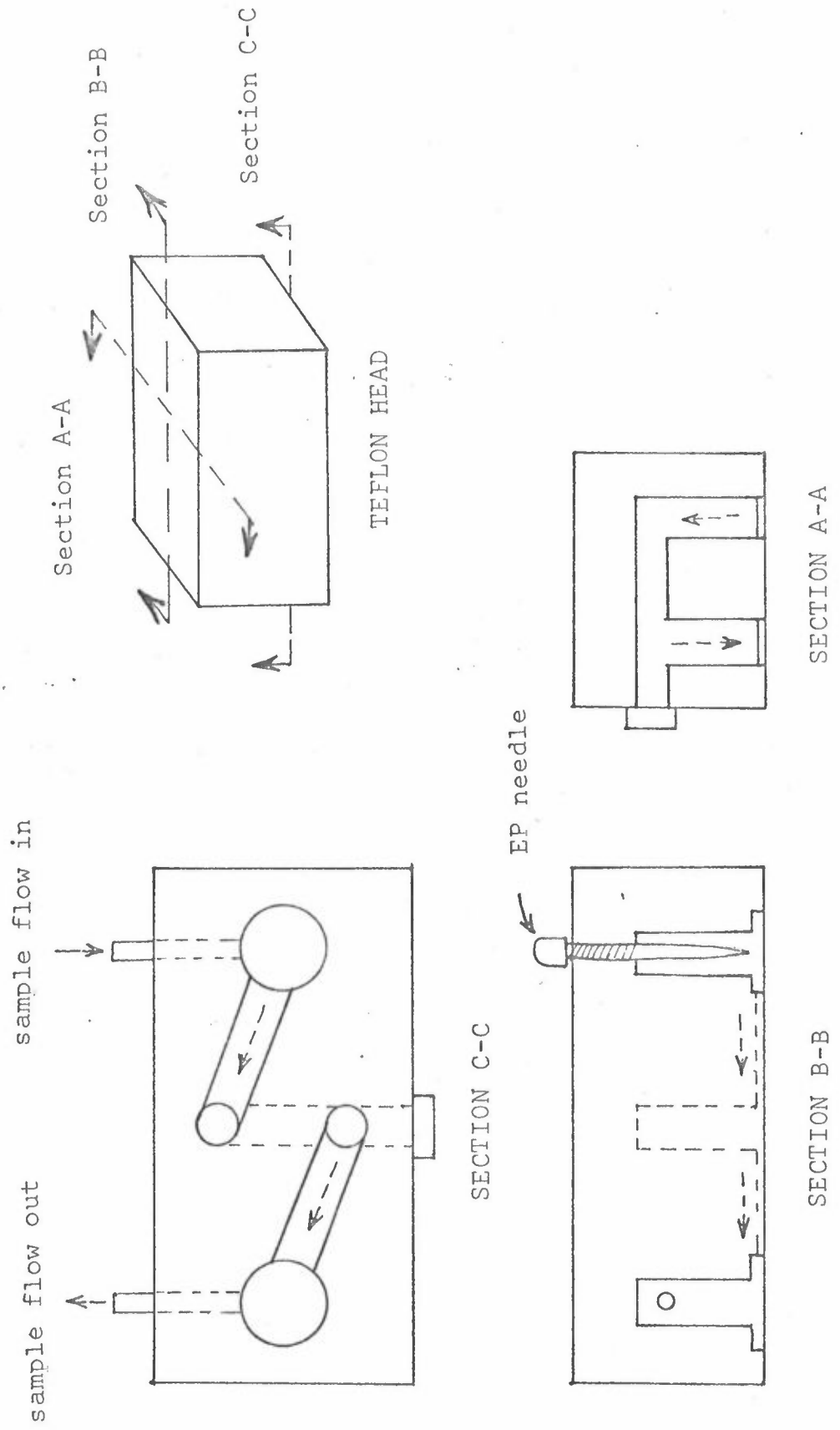

Figure 3-2. PMM Sampling Head

Chapter 4

ELECTRICAL SYSTEM FOR NILU PPM

INTRODUCTION

A simplified block diagram of the Piezoelectric Mass Monitor's electronics is presented in Figure 4-1. Important features of these electronic systems are :

- 12VDC, negative ground operation; reverse- and over-voltage-protection;
- Regulated supplies throughout;
- Less than 2.5A total current requirement;
- Stable operation within 0-70^{o}C and 11.5-15 VDC supply voltages;
- Electrostatic Precipitator current regulated and adjustable 1-15uA; EP voltage ranges between 3-6KVDC;
- Choice of crystals 1-20MHz or greater;
- Displays true beat or preset zero frequencies;
- Periodic sampling at 1, 2, 3 or 6 hour intervals;
- Synchronous data-taping and -decoding on conventional 2 track recorders; recorder start/stop relay;
- Adjustable mass-overload indicator;
- Signal-loss indicator;
- Data-averaging from 1 second to 3000 seconds;
- Low power operational facility for 50% reduction during recorded measurements;
- Switched, regulated power available for air-flow and -heating systems.

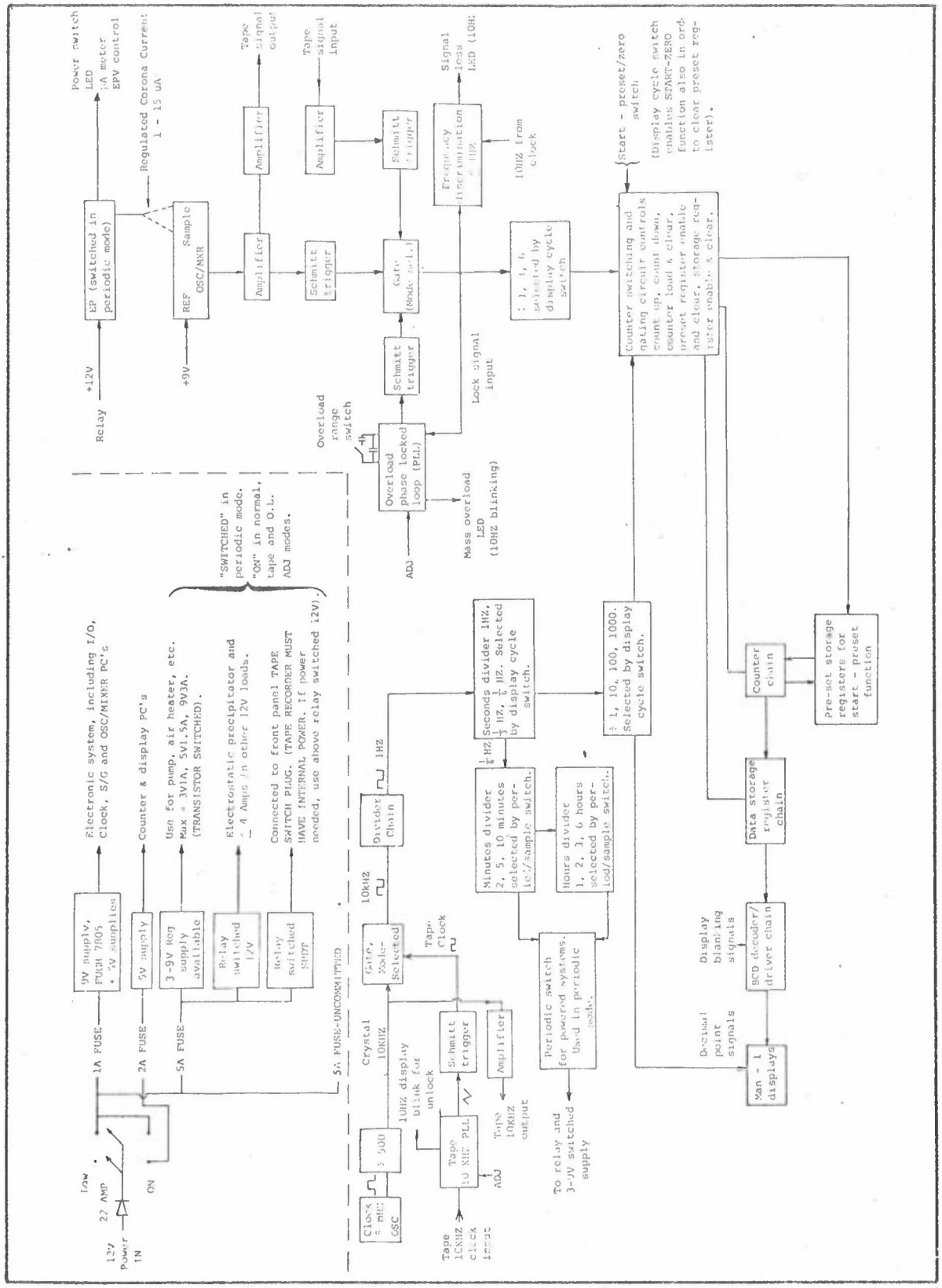

Figure 4-1 Block Diagram of PMM Electronics

POWER REQUIREMENTS

Input Voltage - + 12 VDC (White power lead)
Negative ground (Black power lead)

Minimum Voltage - + 11.5VDC

Maximum Voltage - + 15VDC

DO NOT EXCEED 15VDC FOR EXTENDED PERIOD! (PMM will withstand 35VDC. Absolute maximum for 10 seconds.)

Reverse Voltage Protection - up to Minus 100VDC with 22A diode.

DO NOT BYPASS OR REMOVE 22A REVERSE-VOLTAGE-PROTECTION-DIODE UNLESS POLARIZED POWER PLUG HAS BEEN INSTALLED! (Elimination of this diode will increase running time on 12 volt storage battery.)

Input Current Requirement - 2.4A average with electronics and EP operating

- 0.7A in LOW power-switch position between PERIODIC samples.

DO NOT EXCEED 15A TOTAL LOADING PER CONTACT OF MAIN POWER DPDT SWITCH!

OPERATION

POWER — ON - All systems powered.
LOW - All systems except Counter & Display PC's powered.

START — ZERO - Clears Clock & Counters for PMM turn-on initialization, start of PERIODIC sample series, or to display true crystal beat frequency.

PRESET - Subtracts beat frequency for new zero.

MODE — NORMAL - Used for continuous operation of all systems.

PERIODIC - Switches EP, air-system power and tape recorder for sampling at selected intervals.

TAPE - Connects TAPE SIGNAL inputs to Counter/Display for decoding of synchronized, taped data.

O.L. ADJ. - Connects O.L. PLL to Counter/Display for adjustment of MASS OVERLOAD frequency.

O.L. RANGE — (Located on I/O PC.) Selects high, 12kHz, or low, 2kHz-12kHz, O.L. PLL frequency ranges.

O.L. PLL — Adjusts PLL center frequency to desired MASS OVERLOAD frequency. (Tracking range is approximately ± 1%.)

TAPE PLL — Sets center frequency of 10kHz PLL to accomodate tape recorder speed variations. (PLL will track within ± 5% of adjusted frequency.)

DISPLAY CYCLE	Selects desired sample averaging interval. Changing switch positions enables START-ZERO function momentarily to prepare Clock and Counter for new CYCLE time.
PERIOD/ SAMPLE	Selects desired PERIODIC sampling interval and duration. (Active in PERIODIC MODE only.)
TAPE SIGNAL	Connects signal and synchronization - 10kHz inputs and outputs to tape recorder.
TAPE SWITCH	Connects tape recorder to floating relay SPST switch. (Can be converted to + 12VDC or grounding t/r switch.)
DECIMAL POINT BLINKING	Decimal Point comes on at start of each DISPLAY CYCLE and goes off midway between CYCLES.
DISPLAY BLINKING	Display blinks in TAPE MODE when TAPE PLL is unable to lock onto the taped 10kHz synchronization signal. (Decoding taped PERIODIC samples causes Display Blinking between sample intervals; this is due to the start/stop recording procedure and is useful to mark sample periods.)
MASS OVERLOAD LED	Blinks when beat frequency attains MASS OVERLOAD level ± 1%. Useful for increasing and decreasing frequencies.
SIGNAL LOSS LED	Indicates loss of beat frequency in NORMAL MODE or of taped signal in TAPE MODE.
ON LOW LED	Indicates that PMM is operating when LOW POWER is used and all other LED's are off.

SAMPLING LED	Comes on when PMM is sampling in the PERIODIC MODE.
EP POWER	Switches off EP power when adjustment of Electrode is needed or Crystal Clip-Box is to be removed.
EPV	Adjusts regulated EP current level, 1-15uA.
EPI METER	Registers EP contra current level, 20uA full scale.
F/O	(Located on Crystal Clip-Box.) Gate-switches Crystal Oscillators between Fundamental and Overtone operation.

PMM ELECTRONIC SYSTEMS

The electronics complement to this PMM consists of seven functionally distinct systems, employing 83 integrated circuits and 20 transistors.

1. Power Supplies (Figure 4-2). The main POWER switch controls four parallel, fuse-protected power lines to the PMM systems.

   a) 1-Amp Fuse: Supplies E12V which has 0.7A requirement. E12V powers the Oscillator/Mixer, Input/Output, Clock and Switch/Gate PC's via the E9V regulated analogue supply and the 5V regulators located on the aluminium PC dividers. E12V is "on" in both the ON and LOW power-switch positions.

   b) 2-Amp Fuse: Supplies CD12V which requires 1.2A. CD12V powers the Counter and Display PC's via the regulated CD5V supply and is "off" when LOW power is used.

   c) 5-Amp Fuse: Supplies H12V to one (or both) Relay contact(s) and to the H3-9V adjustable regulated supply. The Relay and H3-9V supply are both electronically switched by the PMM clocking system in the PERIODIC MODE and are always "on" in the NORMAL MODE. The Relay switches the EP power (0.83A Max., 0.7A Typ.) and each Relay contact is rated for 5A Maximum. The second Relay contact is used as a floating SPST switch for a tape recorder start/stop function. Power available to air-systems consists of 1) switched H12V up to 4A using the EP Relay contact, 2) switched, regulated adjustable H3-9V with Maximum power available of 3V1.1A through 5V1.4A through 9V3.3A (Up to 5A is available from H3-9V if sufficient heat-sinking or

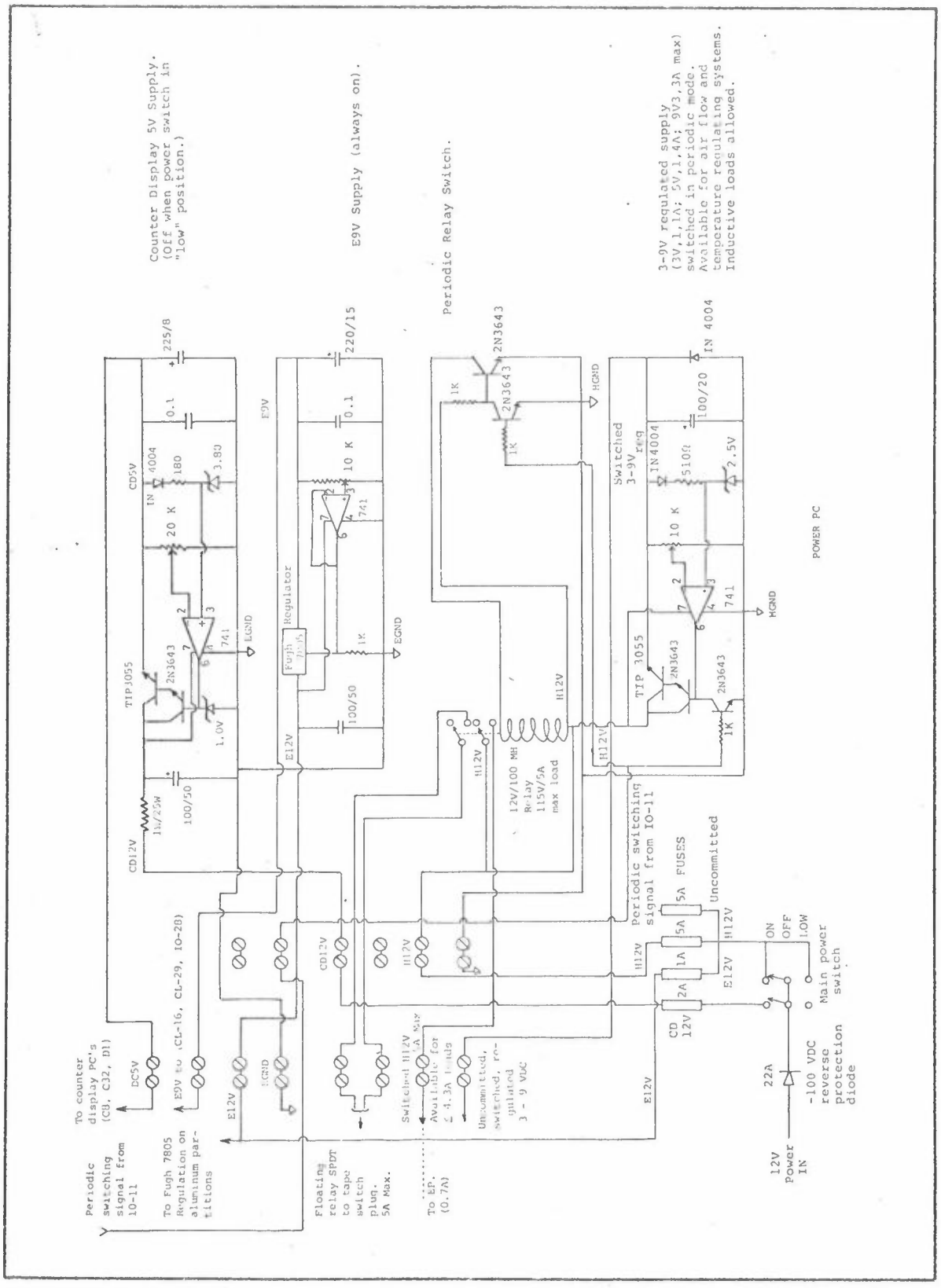

Figure 4-2 PMM Power Supplies

cooling is provided, and 3) up to 5A of H12V from the second Relay contact, if a 12V tape recorder is being used. H3-9V can be safely used with inducive loads.

d) 5-Amp Fuse: Unconnected and uncommitted.

TOTAL PMM CURRENT SHOULD NOT EXCEED 15A MAXIMUM PER POWER-SWITCH-POLE UNLESS SWITCH IS REPLACED. TOTAL CURRENT THROUGH REVERSE-VOLTAGE-PROTECTION-DIODE SHOULD NOT EXCEED 20A. The 5-Amp Fuses can be replaced with larger values, provided Maximum Limits for H3-9V current, Relay contacts, POWER switch and 20Amp diode are carefully observed.

2. Electrostatic Precipitator (Figure 4-3). The EP uses an adjustable current-regulator which controls the EP voltage to compensate for changes in sample-air properties and adjustments of the Corona-Electrode height. The desired corona current is selected using the EPV control and the EPI meter, and is constant, once set, regardless of other factors.

WARNING! TURN OFF EP POWER BEFORE ADJUSTING CORONA-ELECTRODE!

CAUTION! DO NOT VENT OZONE-LADEN SAMPLE AIR INTO THE INSTRUMENT! THIS EP-OZONE CAN QUICKLY OXIDIZE ELECTRONIC CONTACTS.

NOTE! TURN OFF EP BEFORE REMOVING OSC/MXR CLIP-BOX FROM SAMPLE-HEAD! (EP will otherwise try to maintain corona-current by holding maximum high-voltage until the Clip-Box is replaced.)

NOTE! DO NOT RUN EP UNLESS SAMPLES-AIR IS FLOWING! OZONE BUILD-UP CAN OXIDIZE CRYSTAL LEADS AND MAY LEAK INTO CLIP-BOX OR PMM!

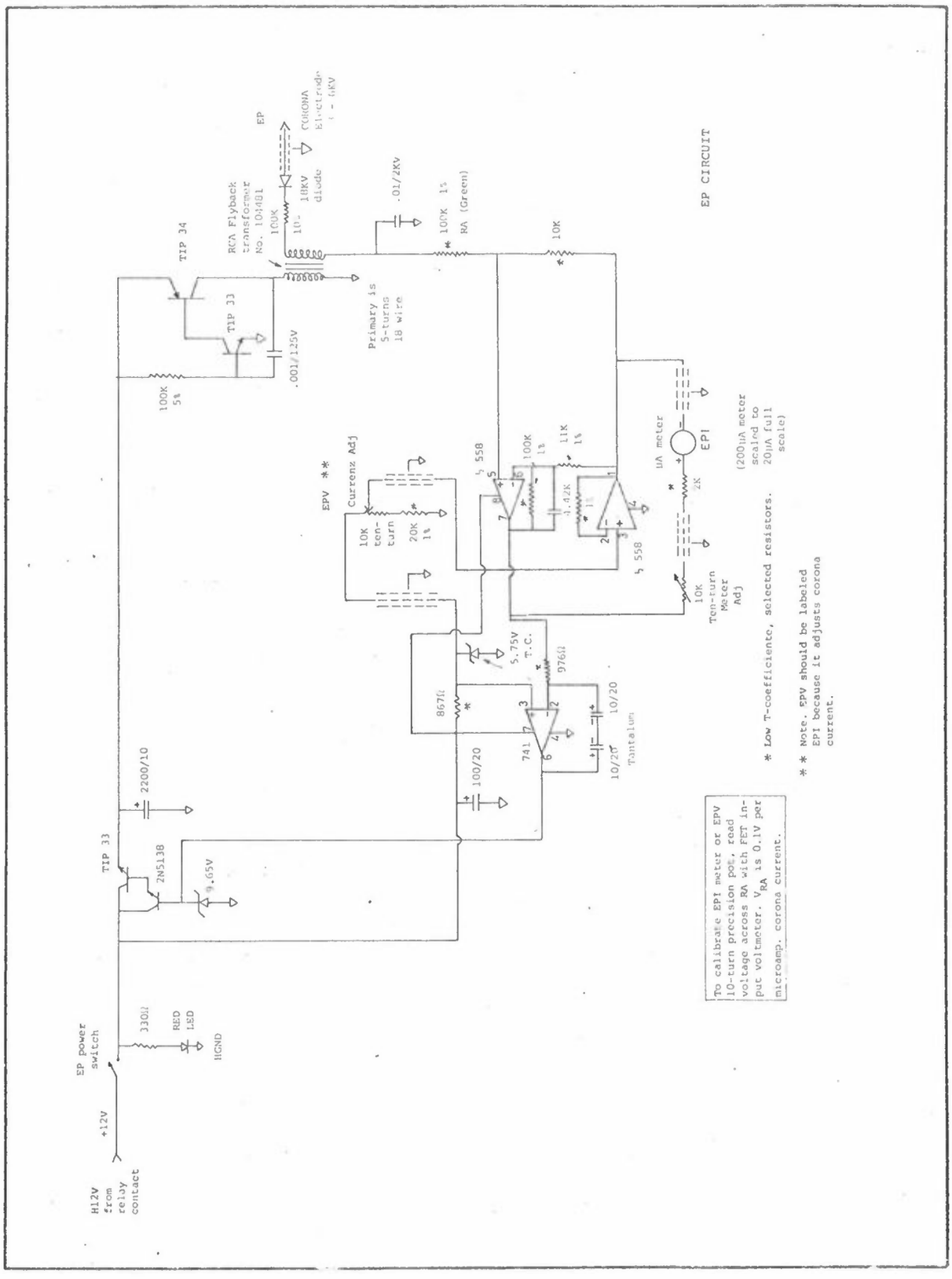

Figure 4-3 PMM Electrostatic Precipitator

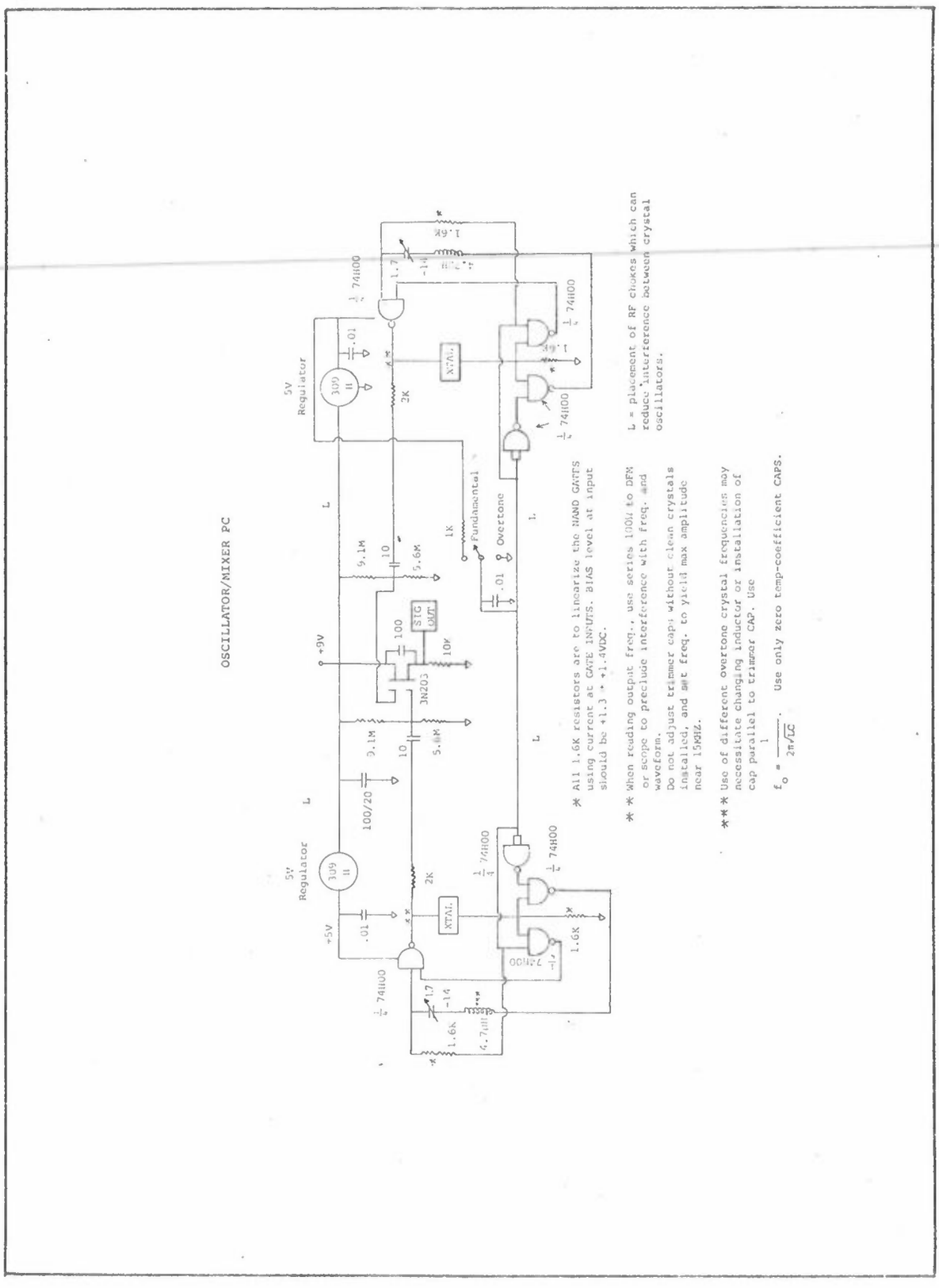

Figure 4-4 Crystal Oscillators & Mixer

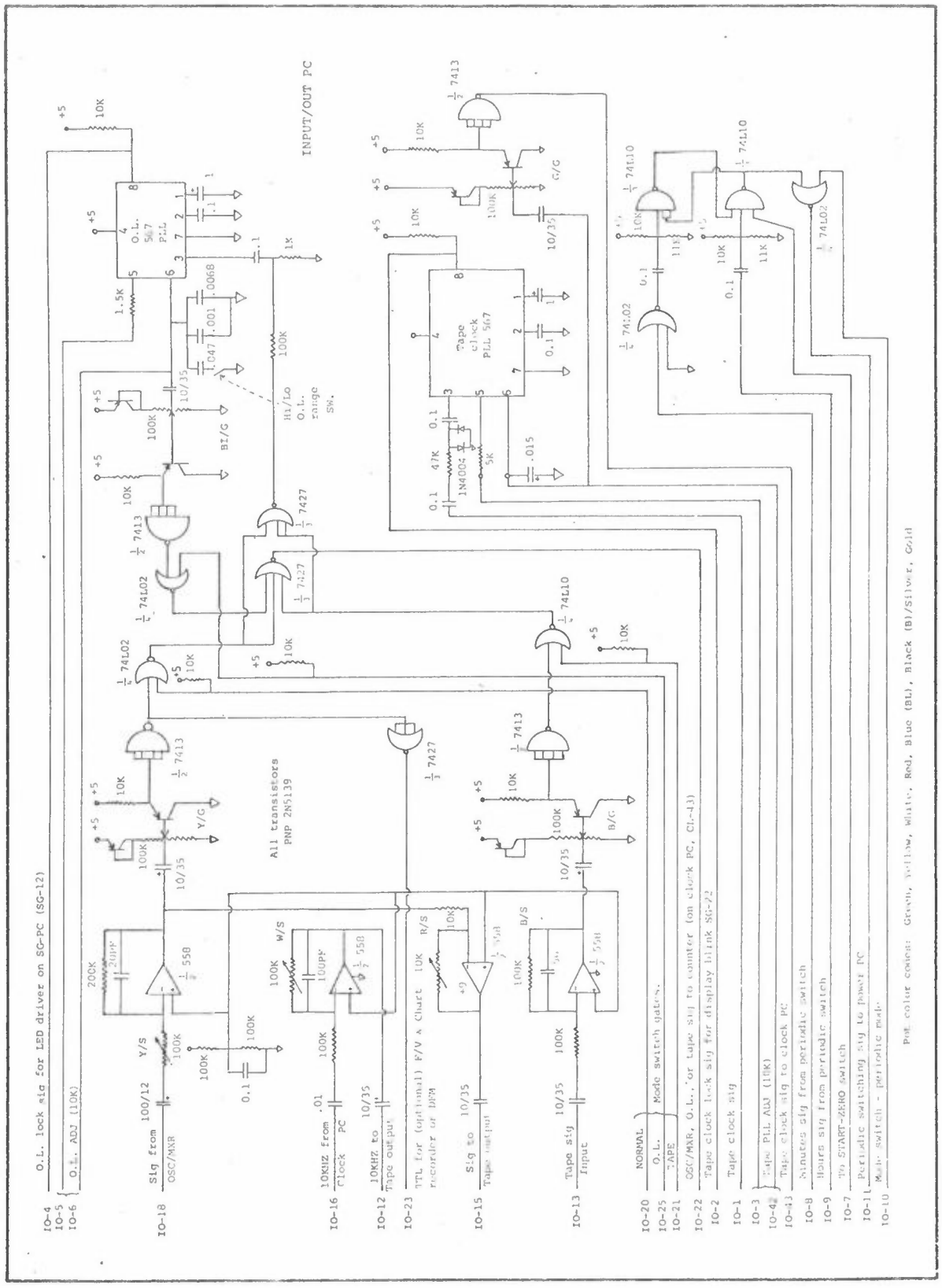

Figure 4-5 Input/Output PC

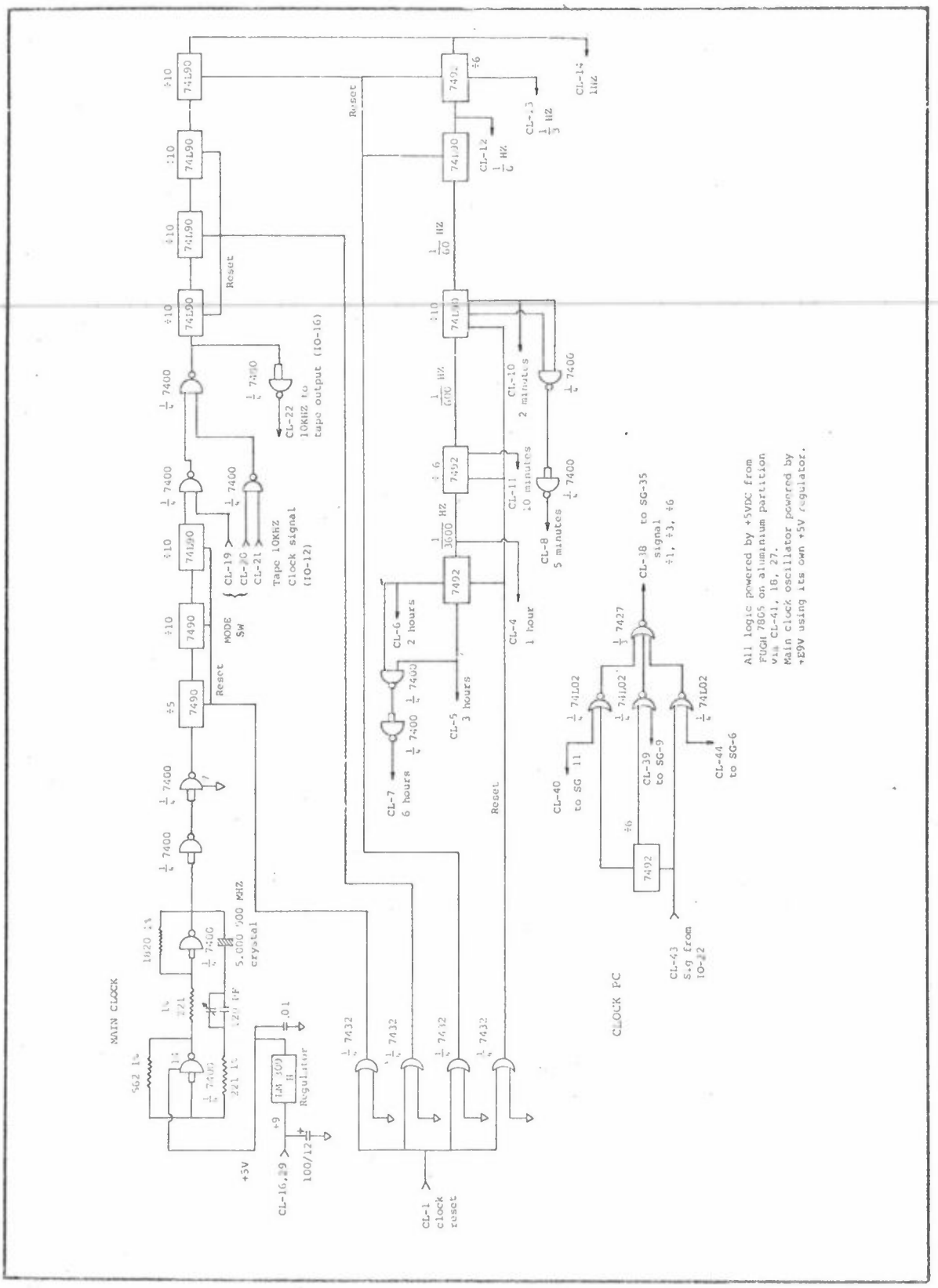

Figure 4-6 Clock PC

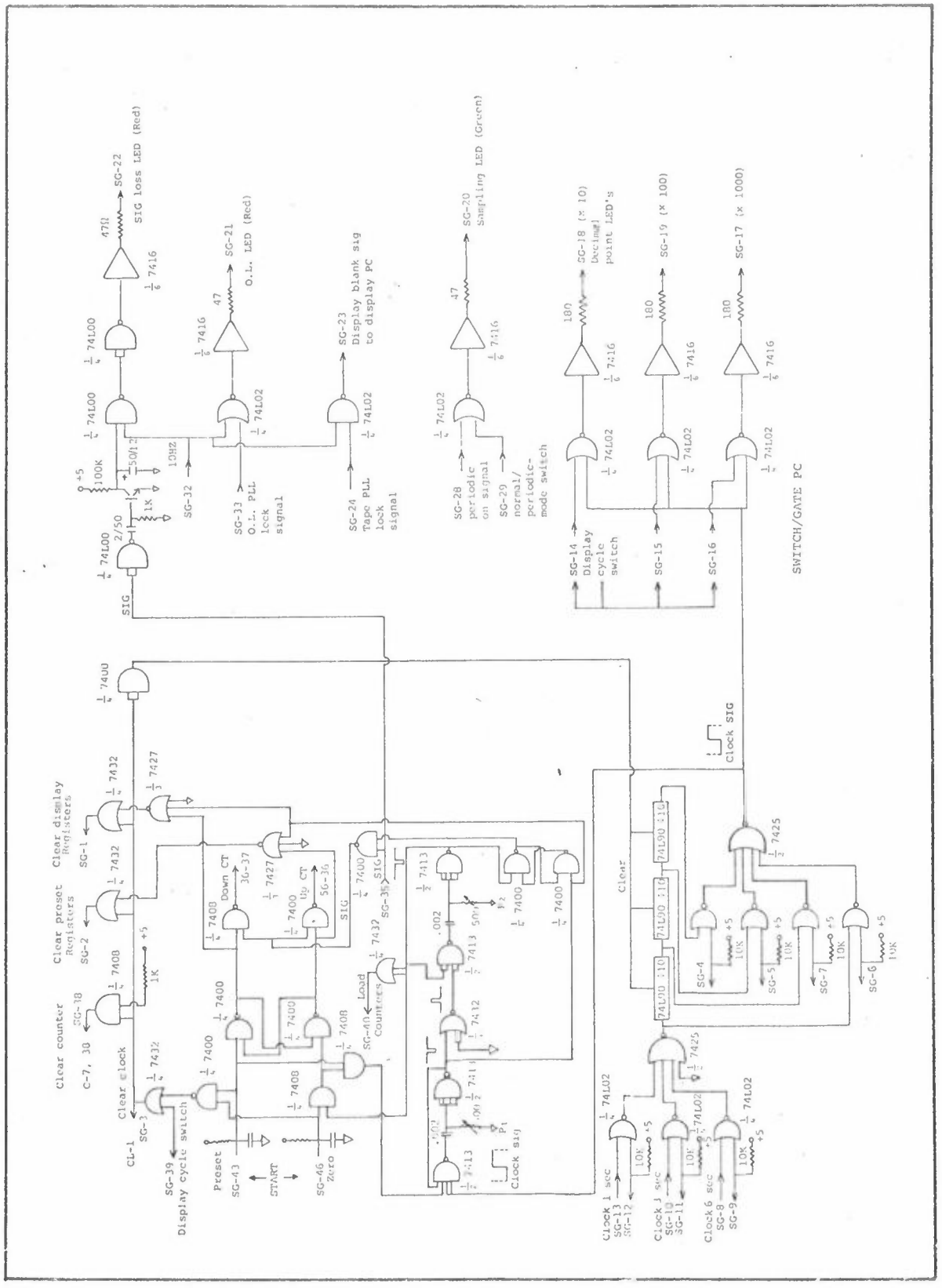

Figure 4-7 Switch/Gate PC

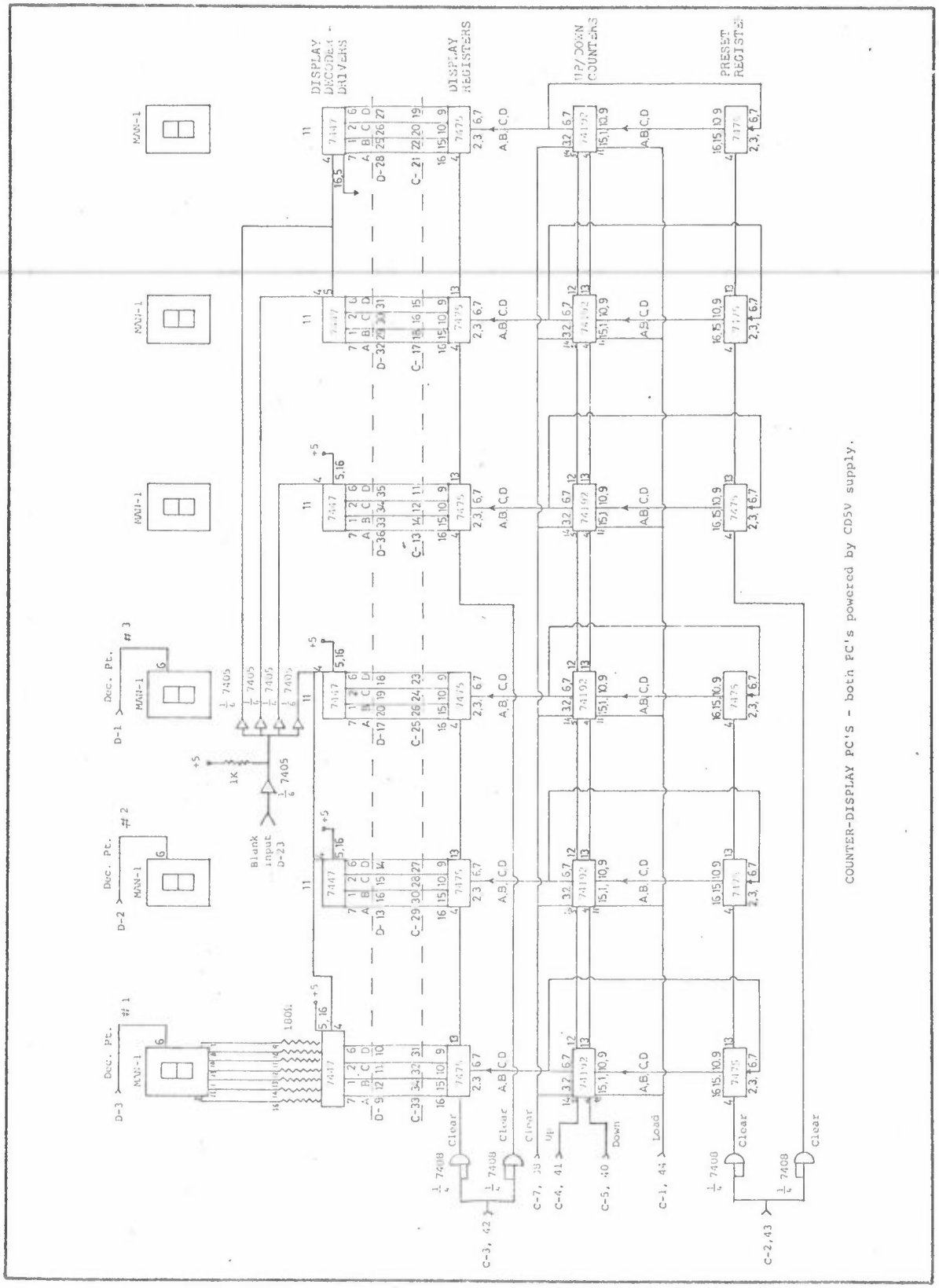

Figure 4-8 Counter & Display PC's

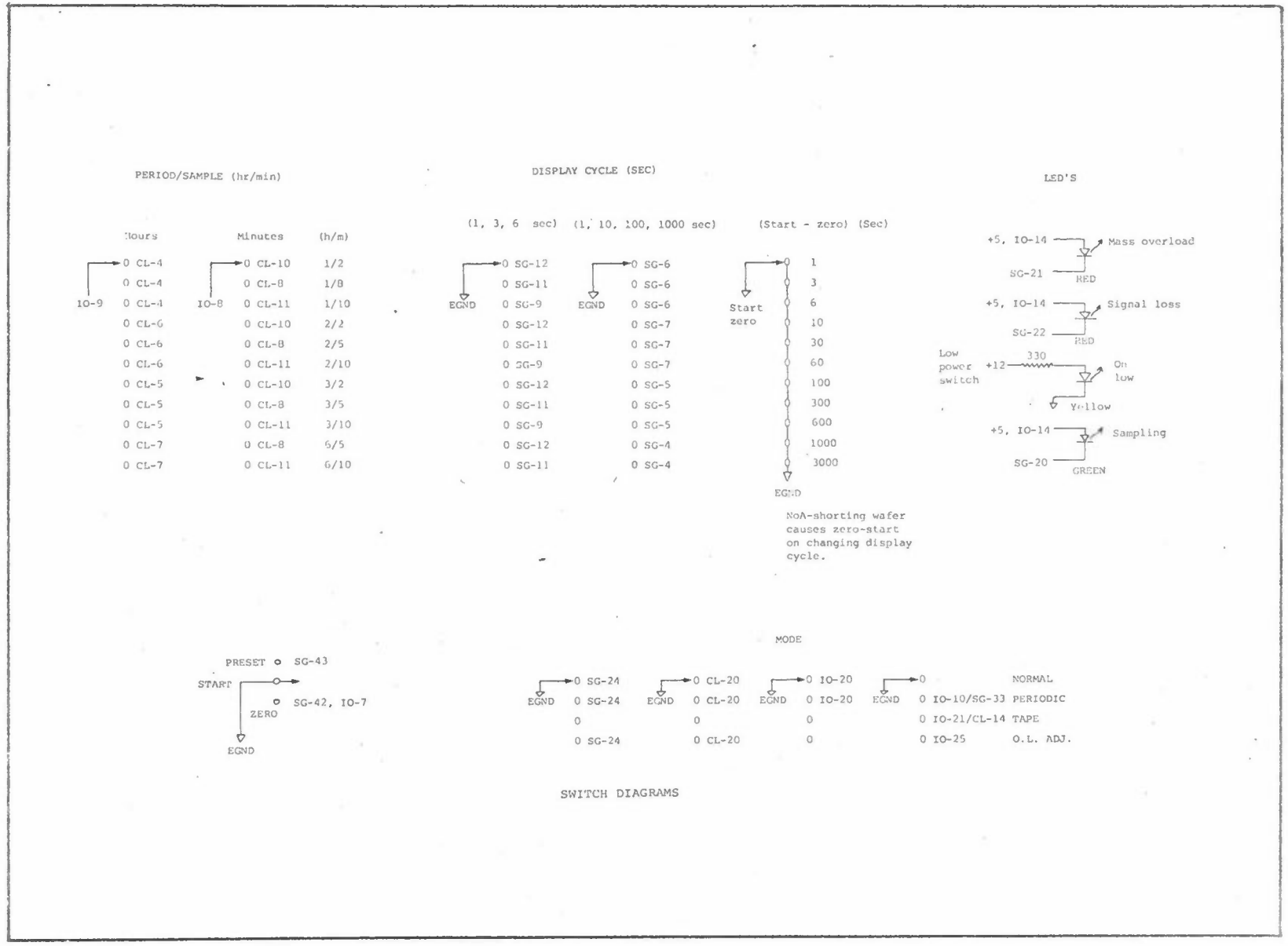

SWITCH DIAGRAMS

Figure 4-9 Switch Diagrams

3. Crystal Oscillators & Mixer (Figure 4-4). The Osc/Mxr PC consists of two 74H00 TTL NAND-Gate crystal oscillators that are Gate-switchable between Fundamental and (LC-tuned) Overtone operation. The mixer is a 3N203 Dual Gate MOSFET operating as a source-follower. The Osc/Mxr PC is powered by E9V and is always operating when the PMM is powered. Crystals of 1-20MHz require readjustment of both oscillators.

4. Input/Output (Figure 4-5)[x] The I/O PC contains amplifiers for Crystal beat-signal. TAPE SIGNAL output and input, TAPE 10kHz and synchronization signal output, and Phase Locked Loops (PLL's) for detection of the TAPE 10kHz input and MASS OVERLOAD frequency.

5. Clock PC (Figure 4-6)[x]. The Clock PC contains the main 5MHz Crystal clocking oscillator and frequency dividers and gates for timing functions.

6. Switch/Gate PC (Figure 4-7)[x]. The S/G PC contains the switching and gating circuitry which controls the Counter PC and gating for other switches, functions and indicators.

7. Counter & Display PC's (Figure 4-8). The CD PC's are powered by CD5V and are "on" only in the ON Power-switch position.

---

x)

These PC's are powered by E12V using E9V and separate 5-volt regulators, and are always operating when the PMM is powered.

SPECIFICATIONS

Electrostatic Precipitator :

EP Regulated Corona Current Range - 1-15uA
EP Voltage - 3KV to 6KV, fixed by current and loading
Operating Frequency - Approximately 29.7kHz
Current Temperature Stability - ± 1% over 0-40°C
Current Load Stability - ± 0.2%

uA Meter - Meter Reading[x)]	True Corona Current
4.2uA	5uA
5.4uA	6uA
6.8uA	7uA
8.0uA	8uA (Cal. Pt.)
10.5uA	10uA
12.7uA	12uA

([x)]Meter non-linearities are the fault of the Meter, not the EP circuitry. See ADJUSTMENTS for calibration proc.)

Oscillators & Mixer:

Usable Crystal Beat-Frequency Range - 100Hz to OVERLOAD
Temperature Stability - Crystal limited

Tape Inputs & Outputs :

Signal Output Amplitude - 0.5V RMS, adjustable
10kHz Output Amplitude - 0.5V RMS, adjustable

Signal Input Amplitude - 0.1 to 4V RMS
10kHz Input Amplitude - 0.15 to 10V RMS

Output Impedances - 300 Ohms, capacitor-coupled
Input Impedances - more than 10k Ohms, capacitor-coupled.

Tape 10kHz PLL:

Tracking Range - ±5% of set frequency

O.L. PLL:

Tracking Range - ±1% of set OVERLOAD frequency

ADJUSTMENTS

EP Meter Calibration:

Connect FET volt-meter across green 100 k 1% resistor at the high-voltage transformer secondary to read the voltage drop due to the corona current. The meter will read 0.1V per microamp. Adjust the miniature 10-turn potentiometer on the EP circuit board until the EP meter reading matches the measured value.

Crystal Oscillator Calibration:

Install new, clean crystals in the oscillators. Connect digital frequency meter and oscilloscope to the oscillator outputs using a series 100 Ohm resistor to isolate them from the oscillators. Adjust the trim capacitors until the correct overtone frequency appears

Clock Oscillator Calibration:

Connect digital frequency meter to the oscillator output to the adjacent 7490 and adjust the trim capacitor for 5.000000MHz.

TAPE PLL Adjustment:

While decoding in the TAPE MODE, adjust the TAPE PLL control to the appropriate center of the region where Display-blinking does not occur. (Blinking occurs between PERIODIC sample decoding, and this control should not be adjusted unless tracking errors are indicated by unexpected Display-blinking. Before changing TAPE PLL, try increasing the 10kHz input amplitude from the tape recorder.)

To return TAPE PLL to 10kHz; 1) Remove TAPE SIGNAL cable from front panel and install a clip-lead from the tape signal output to the tape signal input (top left connector pin to bottom right connector pin); 2) Note crystal beat-frequency displayed in NORMAL MODE; 3) Switch to TAPE MODE and adjust TAPE PLL until blinking display registers approximately the same frequency (±1%). Since the TAPE PLL tracks recorder speed errors of up to ± 5%, exact TAPE PLL settings are not required.

Power Supply Adjustments:

The CD5V, E9V and H3-9V regulated supplies are adjusted using the marked miniature 10-turn potentiometers on the Power Supply PC. The voltages can be monitored at the screw terminals shown in Figure 2.

I/O PC Adjustments:

Fout PNP emitter-followers are located on the I/O PC and are used to level-shift signals to operate 7413 TTL Schmitt trigger IC's. The emitter-lok Ohm junctions of these followers should be 1.4VDC ± 0.05V. The color-coded adjustment potentiometers are :

Yellow/Gold - Oscillator/Mixer input signal
Black/Gold - Tape input signal
Green/Gold - TApe PLL signal
Blue/Gold - O.L. PLL signal

Four variable-gain linear amplifiers are adjusted to the following levels:

Yellow/Silver - Oscillator Mixer input signal, 3V p-p
Black/Silver - Tape input signal, 3V p-p

Red/Silver - Tape signal output, 0.7V p-p
White/Silver - Tape 10kHz output, 0.7V p-p
(The two Tape output amplifiers can be readjusted to match tape recorder requirements.)

WARNING! DO NOT SHORT BLACK POWER-SUPPLY HEAT-SINKS TO CONNECTIONS ON THE I/O PC! HEAT-SINKS ARE AT 12VDC!

Switch/Gate PC Adjustments:

Two 10-turn miniature potentiometers, labelled P1 and P2, are located on the S/G PC and are used to adjust the width of timing pulses for the Counter PC. Pulse widths should be approximately 1 microsecond. To adjust, back-off potentiometers until display ceases to operate (using START ZERO to check, since the display will hold the last number when counting ceases) and advance potentiometers until approximately 1½ turns beyond the point where the Counter begins working. P1 and P2 should be adjusted separately, using the above procedure. This adjustment should not be made, unless trouble occurs and only after eliminating possible causes elsewhere.

RECOMMENDATIONS

1. If a 1-20MHz fundamental and overtone operational capability is not considered important, the TTL crystal-oscillators can be replaced with transistor LC-tuned overtone oscillators having lower drive levels and minimal harmonic content. The high drive and fast switching speed of the TTL oscillators cause sufficient interaction to produce locking onto zero beats near 40-80Hz. Some, if not most, of this interaction can be eliminated with improved RF isolation between 5V oscillator regulators and the mixer and between gate-switch connection (the O/F switch is common to both oscillators.)

2. The uA meter for the EP corona-current is not linear and can be replaced, unless repeatability is the only concern. A better solution is to install a miniature 10-turn decade dial on the EPV control. The EPV potentiometer is highly linear and can be calibrated to obtain precisely repeatable current settings without reference to the uA meter.

3. Future crystal electrodes and clip-leads should be gold- not nickel-plated, since corrosion from EP-ozone is a serious problem. Also, the clip-leads should be rigidly attached to the crystal electrode (using baked cement as with sealed crystal units), in order to guarantee good electrical contact and crystal-centering. Finally, a firm, non-conducting support beneath the crystal running between, and attached to, clip-lead pins would serve to space the crystal above the teflon base and facilitate rapid crystal changes by plugging and unplugging the crystal and mounting as a unit. Notches in the teflon base or plastic support would accomodate a pulling-tool made for the purpose.

4. A polarized power-plug should be installed and the 20A diode removed.

5. If a chart-recorder output is desired, the following ought to be considered : A frequency-to-voltage converter (f/v) can be purchased commercially on a single IC for less cost than a D/A and does not require that the Counter PC be operating. The f/v would simply monitor the oscillator frequency at the I/O PC, which is always operating when the PMM is powered. An f/v would probably require less power, would certainly require fewer connections (one versus 24), but may not be available with sufficient linearity or temperature stability for use here. The D/A would require that the Counter PC is operating continuously, since to switch the Counter in the PERIODIC MODE would cause spurious stored counts to appear unless the ZERO START function is enabled each time. If a D/A is preferred, it may be desirable to modify the power switch such that the LOW position powers the Counter, but not the Display. (Note, the CD5V supply is very stable and reliable and should be used for the C and D PC's, and carefully adjusted to 5V. Also, in the present configuration it is not possible to check the beat frequency in LOW PERIODIC operation without destroying the clock timing. This could be remedied by running the Counter continuously and connecting the Display to one relay contact, powering both by CD5V; the relay contact would not then be available for other use, however.)

PARTS LIST

Oscillator/Mixer PC :

2 - SN74H00 Quad NAND Gate TTL Integrated Circuits
1 - 3N203 Dual Gate MOSFET
2 - LM309H, 200 ma, 5 Volt Regulator IC's
2 - 1.7-14pF Trim Capacitors
4 - 0.01uF/50V Disc Capacitors
2 - 10 pF NPO (Zero Temp Coeff) Capacitors
1 - 100uF/20V Tantalum Electrolytic Capacitor
2 - 2k Ohm, 2% Resistors (All Resistors are Low Wattage types)
4 - 1.6k Ohm, 2%, LOW TC Resistors
2 - 9.1MegOhm, 10% Resistors
2 - 5.6MegOhm " "
1 - 10kOhm " "
1 - 1kOhm " "
1 - SPDT Miniature Toggle Switch
1 - Pair 3-Prong Miniature Series Molex Nylon Sockets, Male and Female.

Electrostatic Precipitator:

1 - RCA Hi-Voltage & Horizontal Output Transformer (Flyback for TV), 22KV, No. 104481 (HO-290). (5-turns No. 18 wire for primary winding.)
1 - 18KV Diode
1 - uA Meter, 200uA Movement (Scaled to 20uA Full Scale), Calectro Cat. No. D1-907.
2 - TIP 33 NPN Transistor, Texas Instruments
1 - TIP 34 PNP Transistor
1 - 2N5128 NPN Transistor
1 - 5558 Dual Operational Amplifier IC
1 - 741 Operational Amplifier IC
1 - 2200uF/10V Electrolytic Capacitor

1 - 100uF/20V Tantalum Electrolytic Capacitor
2 - 10uF/20V " " "
1 - 0.001uF/125V Polystyrene Capacitor
1 - 0.01uF/2KV Disc Capacitor
1 - 0.01uF/50V " "
1 - 867 Ohm, 1/4W, 1% Resistor
1 - 20kOhm " " "
2 - 100kOhm " " "
1 - 976 Ohm " " "
1 - 4.42kOhm " " "
1 - 11kOhm " " "
1 - 220kOhm, 10% 1/4W Resistor
1 - 10kOhm, 2% " "
1 - 100kOhm, 10% " "
1 - 300 Ohm " "
1 - 5.75V, Temperature Compensated Zener
1 - 9.65 Zener, uncompensated
1 - LED, 110ma, RED
1 - SPST Miniature Toggle Switch, 1A

Display PC:

6 - MAN-1 Seven-Segment LED Display Packages
6 - 7447 TTL BCD-To-Seven-Segment Decoder/Drivers
1 - 7405 TTL Hex Inverters (Open collector output)
1 - 1kOhm, 10%, 1/4W Resistor
42 - 180 Ohm, 10%, 1/4W Resistor

Counter PC:

6 - 74192 TTL Synchronous 4-Bit Up/Down Counters with Preset Inputs
12 - 7475 TTL 4-Bit Bistable Latches
1 - 7408 TTL Quad 2-Input Positive AND Dates
1 - 100uF/12V Electrolytic Capacitor
1 - 0.22uF/75V Mylar Capacitor
15 - 0.01uF/50V Disc Capacitors

Switch/Gate PC:

3 - 7400 TTL Quad 2-Input Positive NAND Gates
2 - 7402 TTL Quad 2-Input Positive NOR Gates
1 - 74L02 TTL Quad 2-Input Positive NOR Gates, Low Power
2 - 7413 TTL Dual NAND Schmitt Triggers
1 - 7416 TTL Hex Inverter Buffers/Drivers
(Open Collector Outputs)
1 - 7425 TTL Dual 4-Input NOR Gates with Strobe
1 - 7427 TTL Triple 3-Input Positive NOR Gates
1 - 7408 TTL Quad 2-Input Positive AND Gates
1 - 7432 TTL Quad 2-Input Positive OR Gates
3 - 74L90 TTL Decade Counters
1 - 2N3643 NPN Transistor
1 - 100uF/12V Electrolytic Capacitor
1 - 33uF/16V " "
1 - 50uF/12V " "
2 - 0.002uF Polystyrene Capacitors
2 - 0.01uF/50V Disc Capacitors
2 - 500 Ohm, 10-Turn Potentiometers, 50 ppm/^{o}C
12 - 10kOhm, 10% 1/4W Resistors
2 - 1kOhm, 10% " "
1 - 100kOhm, 5% " "
1 - 2uF/50V Electrolytic Capacitor
3 - 47 Ohm, 10%, 1/4W Resistors
3 - 180 Ohm, 10% " "

Clock PC:

1 - LM309H, 200ma, 5 Volt Regulator IC
3 - 7400 TTL Quad 2-Input Positive NAND Gates
1 - 74L02 TTL Quad 2-Input Positive NOR Gates, Low Power
1 - 7427 TTL Triple 3-Input Positive NOR Gates
1 - 7432 TTL Quad 2-Input Positive OR Gates
2 - 7490 TTL Decade Counters
7 - 74L90 TT Decade Counters, Low Power
4 - 7492 TTL Divide-by-Twelve Counters
1 - 5.000000MHZ Crystal
1 - 1-10pF Trimmer Capacitor
1 - 120pF NPO (Zero Temp Coeff) Capacitor
9 - 0.01uF/50V Disc Capacitors
2 - 100uF/12V Electrolytic Capacitors
2 - 220 Ohm, 1%, 1/4W Resistors, 20 ppm/°C
1 - 560 Ohm, 1%, 1/4W Resistors, 20 ppm/°C
1 - 1820 Ohm, 1%, 1/4W Resistors, 20 ppm/°C

Input/Output PC:

2 - 558 Dual Operational Amplifiers
2 - 567 Tone Decoder Phase Locked Loops
2 - 7413 TTL Dual NAND Schmitt Triggers
2 - 74L02 TTL Quad 2-Input Positive NOR Gates, Low Power
1 - 74L10 TTL Triple 3-Input Positive NAND Gates
1 - 7427 TTL Triple 3-Input Positive NOR Gates
8 - 2N5139 PNP Transistors
1 - 100uF/12V Electrolytic Capacitor
7 - 10uF/35V Electrolytic Capacitors
2 - 1uF/12V Electrolytic Capacitors
6 - 0.1uF/100V Mylar Capacitors
1 - 0.22uF/75V Mylar Capacitor
1 - 0.047uF/100V Mylar Capacitor
2 - 0.1uF/50V Disc Capacitors
1 - 20pF Disc Capacitor
1 - 56pF Disc Capacitor

1 - 100pF Polystyrene Capacitor
1 - 0.015uF Polystyrene Capacitor
1 - 0.0068uF Polystyrene Capacitor
1 - 0.001uF Polystyrene Capacitor
2 - 1N4004 Diodes
1 - SPDT Miniature Slide Switch
1 - 10kOhm Miniature 1-Turn Trim Potentiometer
7 - 100kOhm Miniature 1-Turn Trim Potentiometers
1 - 200kOhm, 5%, 1/4W Resistor
2 - 100kOhm, 5%, 1/4W Resistors
12 - 10kOhm, 5%, 1/4W Resistors
2 - 11.8kOhm, 2%, 1/4W Resistors
1 - 47kOhm, 5%, 1/4W Resistor
1 - 5kOhm, 1%, 1/4W Resistor
1 - 1.5kOhm, 2%, 1/4W Resistor

Power Supply PC :

3 - 741 Operational Amplifiers
4 - Fugh 7805 5-Volt Regulators, 1 Amp. (one located on Power PC, three located on Aluminium Dividers.)
2 - TIP3055 NPN Power Transistors
5 - 2N3643 NPN Transistors
1 - 6.1V Zener, ½W
1 - 3.8V Zener, ½W
1 - 2.5V Zener, ½W
3 - 1N4004 Diodes
1 - 22Amp. Diode, Motorola HEP R01 01, 100PIV (Near Main Power Switch)
1 - DPDT Miniature Relay, 12V/100ma input, 125V/5V Maximum Load
3 - 4-Section Screw Terminal Strips
1 - 2-Section Screw Terminal Strip
4 - Fuseholders (Back Panel)
2 - Fuses, 5 Amp., Type 3AG
1 - Fuse, 2 Amp., Type 3AG
1 - Fuse, 1 Amp., Type 3AG

1 - DPDT On-Off-On Toggle Switch, 15Amp/125V (Front Panel)
2 - 100uF/50V Electrolytic Capacitors
2 - 0.1uF/50V Disc Capacitors
1 - 225uF/8V Electrolytic Capacitor
1 - 220uF/15V Electrolytic Capacitor
1 - 100uF/20V Tantalum Capacitor
1 - 1 Ohm/25 Watt Resistor
2 - 10kOhm/10-turn Potentiometers, 50 ppm/°C
1 - 20kOhm/10-turn Potentiometer, 50 ppm/°C
1 - 180 Ohm, 1%, 1/4W Resistor
1 - 510 Ohm, 1%, 1/4W Resistor
4 - 1kOhm, 5%, 1/4W Resistors
2 - 10 Watt Aluminium Heat Sinks, Black

Miscellaneous :

1 - 330 Ohm, 10%, 1/4W Resistor (On Main Power Switch for "ON LOW" LED)
1 - Amphenol 2-Conductor Male & Female Connector Plug (TAPE SWITCH PLUG)
1 - Amphenol 4-Conductor Male & Female Connector Plug (TAPE SIGNAL)
2 - 10kOhm/10-turn Potentiometers, Panel Mounting (TAPE & O.L. PLL's)
1 - 4P4T Rotary Switch (MODE)
2 - 3P11T Rotary Switches (PERIOD/SAMPLE & DISPLAY CYCLE Switches)
1 - SPST Spring Toggle Switch (START Switch)
2 - 100ma, RED LED's (Front Panel)
1 - 40ma, Yellow LED " "
1 - 40ma, Green LED " "
1 - 2-Section Screw Terminal Strip (Near Main Power Switch)

Addenda

1) All PC pins are clockwise from TOP Right looking at maze and wires on PC package

44..1
43..2
.....
.....

2) To remove PC package
- employ large white connectors to Panel switcher
- Remove top wing nuts
- Remove screw terminal connection, don't forget groyne

(Don't tighten wing nuts beyond finger tight).

- remove carefully, lifting towards back of PMM.

3) To remove whole PMM electronics plus power supplier (i.e. Aluminium platforms)
- disconnect power leader from screw terminal that go to and from Al-platform
- remove white connector to panel switcher
- remove fron two screws below LED's.
- Remove two screws on Al-platform at BACK.
- Slide back and

4) uA-meter workings can be removed without removing plastic fron etc. by removing RED TAPE around nuts.

5) Don't remove a PC unless top wing nuts are loosened.

6) Note that Counter must run continuously (0.6A) if D/A is to be used or you want to be able to check Beat during low periodic. To check beat, can just turn on display

Chapter 5

LIMITATIONS

Errors can and usually do occur with any type of measurement method. The PMM is no exception to this. A number of investigators have reported unexplained errors while using piezoelectric crystals under various conditions (1-6). If these errors can be further identified then they constitute known limitations for the measurement method. In some cases the bias may be evaluated and corretions made. This chapter summarized the type and nature of the errors and subsequent limitations involved. These must be kept in mind when using any PMM instrument including the one built for NILU.

Several types of errors can occur : temperature influence, humidity influence, pressure influence, particle collection characteristics, response linearity and crystal mass sensitivity. The following sections discuss these effects.

Temperature

Daley and Lundgren (6) tested both the Thermo-Systems (TSI), and Celesco instruments, which were described in Chapter 2. It was found in both instruments that the crystal chamber temperature remained constant while the inlet air temperature was varied cyclically. Temperature measurements at various positions in the flow stream indicated that the attenuation of the thermal pulses occurred as the air passed over and around the test crystal. This placed the test crystal in a rather strong and changing thermal gradient and consequently caused an increase in the observed temperature coefficient of nearly an order or magnitude. The effective temperature coefficients, based on the inlet temperature, were 0.9 and 8.7 Hz/^{o}C for the TSI and Celesco

instruments respectively. Using these values they calculated that respective temperature change rates of 0.3 and 1.0°C/min. would be required to produce an error of 5 $\mu g/m^3$. Since temperature change rates higher than these are usually of short duration, they may be eliminated by placing a heat sink in the inlet air stream. A short piece of tubing, preferably a thermal conductor, was found to be satisfactory for this purpose.

Thus, the reference crystal did not effectively compensate for inlet temperature fluctuations because it was not in the same thermal environment as the test crystal, but the resulting error could be effectively reduced by minimizing the inlet temperature change rate.

Humidity

Inertial impactors generally require the use of the surface coating material to assure adhesion of rigid particles. This is true for the Celesco device and for this reason the Daley and Lundgren (6) ran humidity response tests with the electrodes of both the test and reference crystals coated with silicone grease. A typical response curve for clean crystals in the Celesco unit is shown in Figure 5-1. The shape and slope of this response varied somewhat from run to run but in no case was the absolute value of the slope greater than the 0.2 Hz/% shown in the figure. Using this maximum value the error curve shown in Figure 5-2 was calculated. It is clear from this figure that humidity presents little problem with clean, coated crystals in the Celesco unit.

The platinum electrode crystals provided with the TSI unit showed wide variation in humidity response. This variation was due to the action of the corona on the test electrode. New crystals changed frequency approximately 100 Hz for a relative humidity change of 0 to 95%. For used crystals this number increased to over 400 Hz. At a relative humidity of

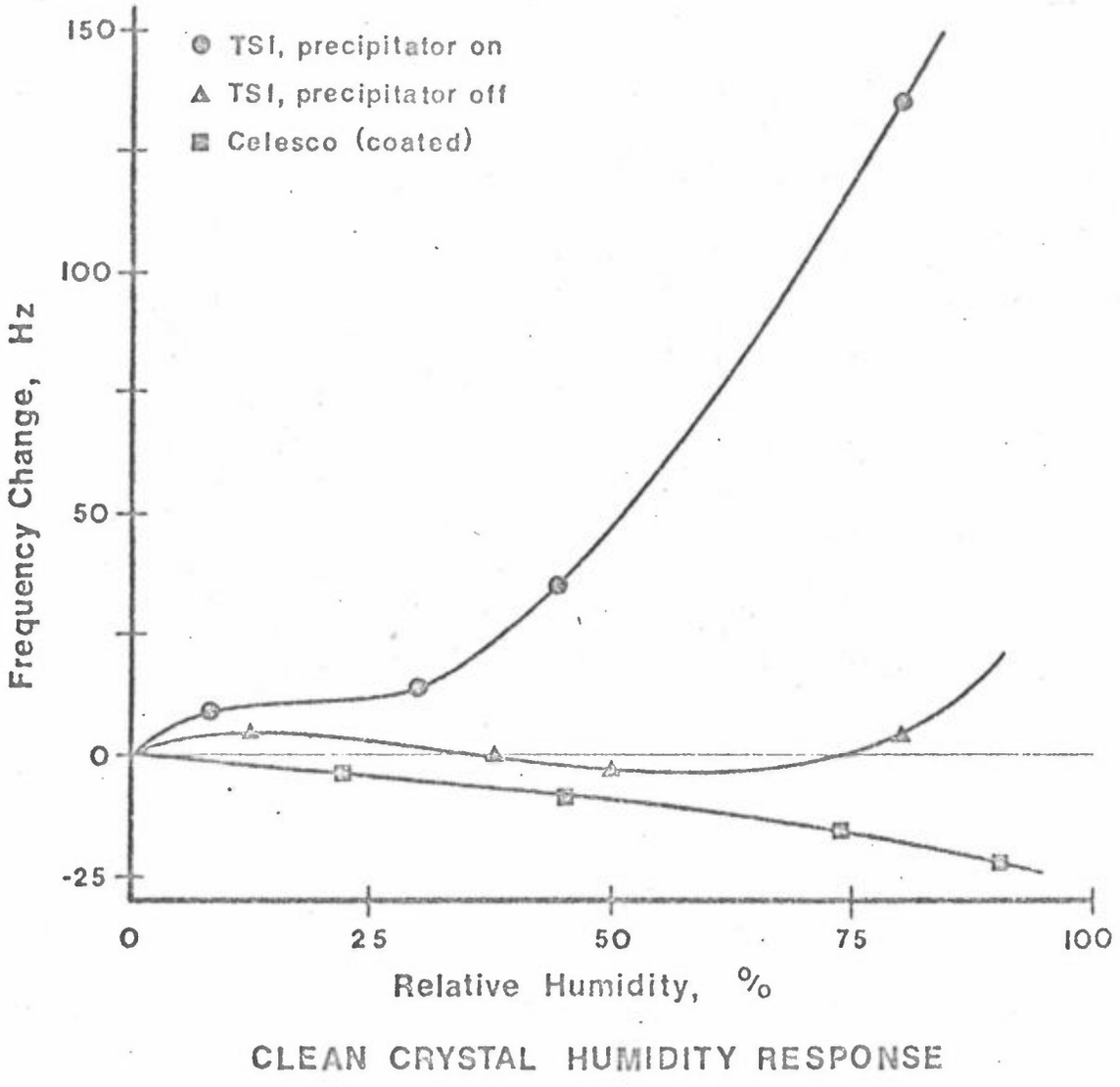

Figure 5-1. Instrument Responses to Inlet Air Stream Relative Humidity Changes in the Absence of Aerosols (After Reference 6)

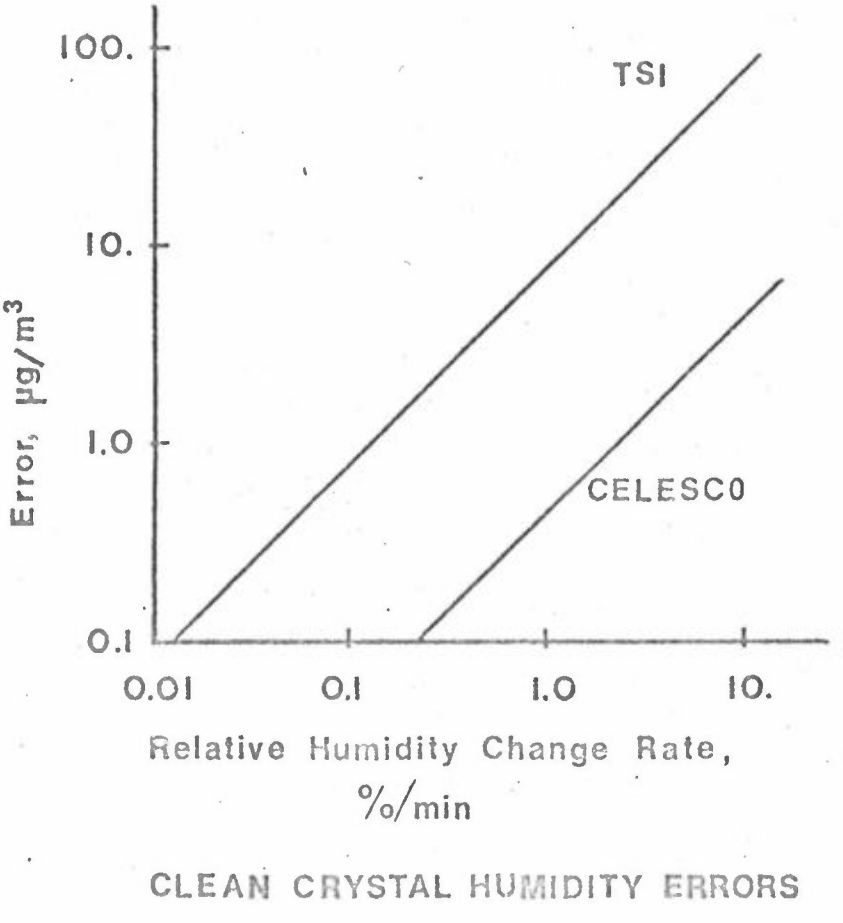

Figure 5-2. Errors Resulting from Inlet Air Relative Humidity Changes in the Absence of Aerosols (After Reference 6)

85% a use period of about 4 hours was required to achieve a steady-state humidity response. The maximum slope of the frequency-time curve during this conditioning period was approximately 4 Hz/min (equivalent to ≈ 20 $\mu g/m^3$). Cleaning the crystal reduced the humidity response, but not to its original value. The change in humidity response caused by the corona means that the reference crystal cannot compensate for humidity fluctuations. This is shown in Figure 5-1. The problem is especially severe for relative humidities greater than 30%. The slope of the "precipitator on" at 40% RH is approximately 1.6 Hz/%. This value was used to calculate the error curve in Figure 5-2. Electrodes coated with a thin layer of silicone grease (≈ 0.5 µm)appeared to reduce the problem and were stable under the corona, but a more thorough evaluation is required to be conclusive.

The moisture affinity of various aerosol deposits was determined by passing air of different relative humidities over a particle laden crystal; the particle collection mechanism was turned off. Results were corrected for the response of the crystal without the deposit. Data obtained for many materials, shown in Figure 5-3 are in good agreement with data obtained by other techniques (7, 8). Measurements obtained using both the TSI and Celesco units were in good agreement.

Humidity induced errors due to the change in deposit mass were calculated for 4 different conditions and the results are shown in Figure 5-4. The crystal loading is expressed in min · $\mu g/m^3$, i.e. the aerosol concentration, sampling time product. These errors are fundamental to the technique and are independent of the instrument used. It should be noted that loadings of 10^4 min · $\mu g/m^3$ are beyond the linear response limits for several tested aerosols (see Figure 5-5).

In ambient air, humidity change rates of 0.5 to 1.0%/min may persist for many minutes, particularly near sunrise or sunset. Change rates much greater than 1%/min may occur for short

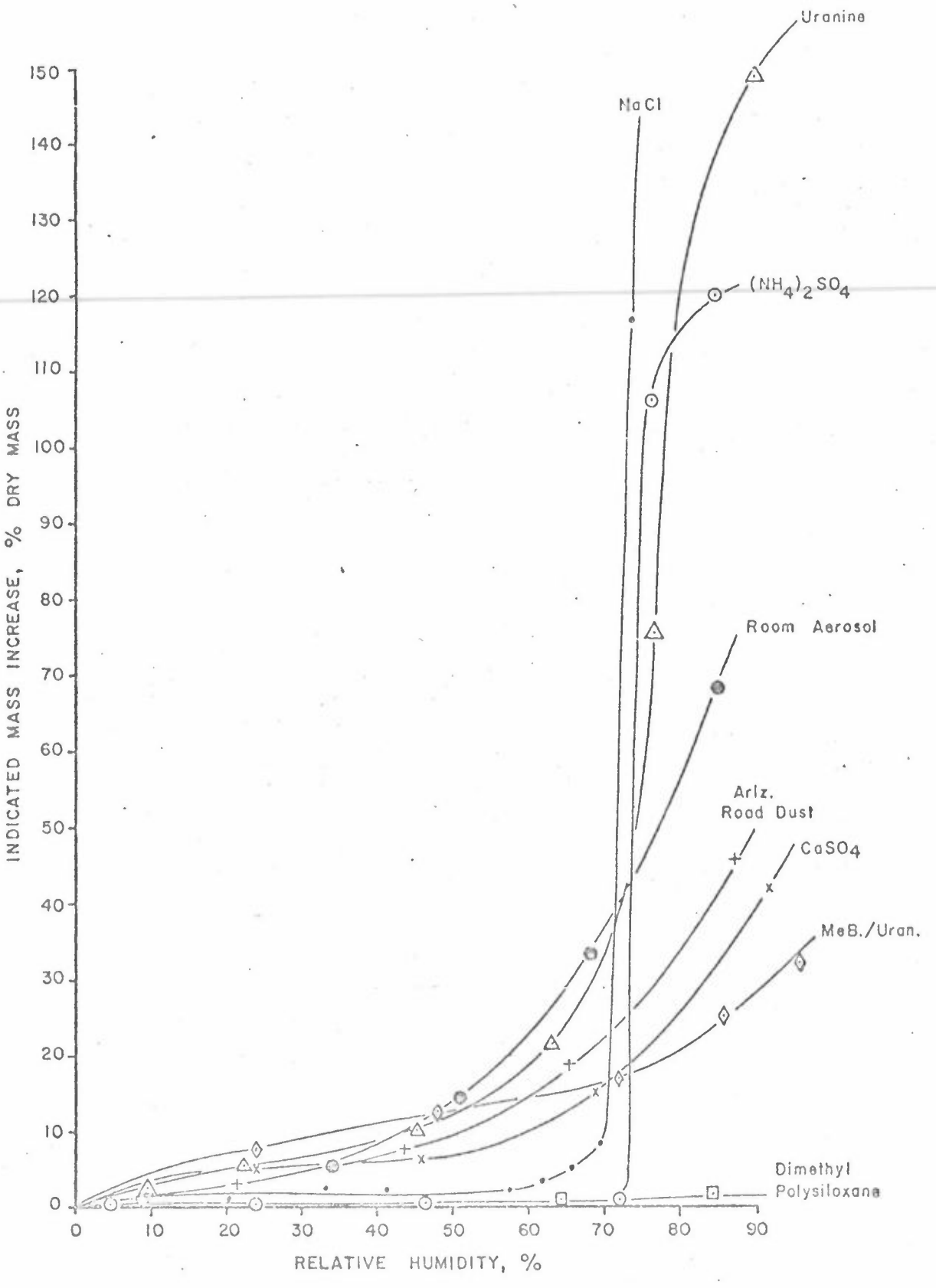

Figure 5-3. Hygroscopicity of Various Materials Deposited on the Crystal Surface (After Reference 6)

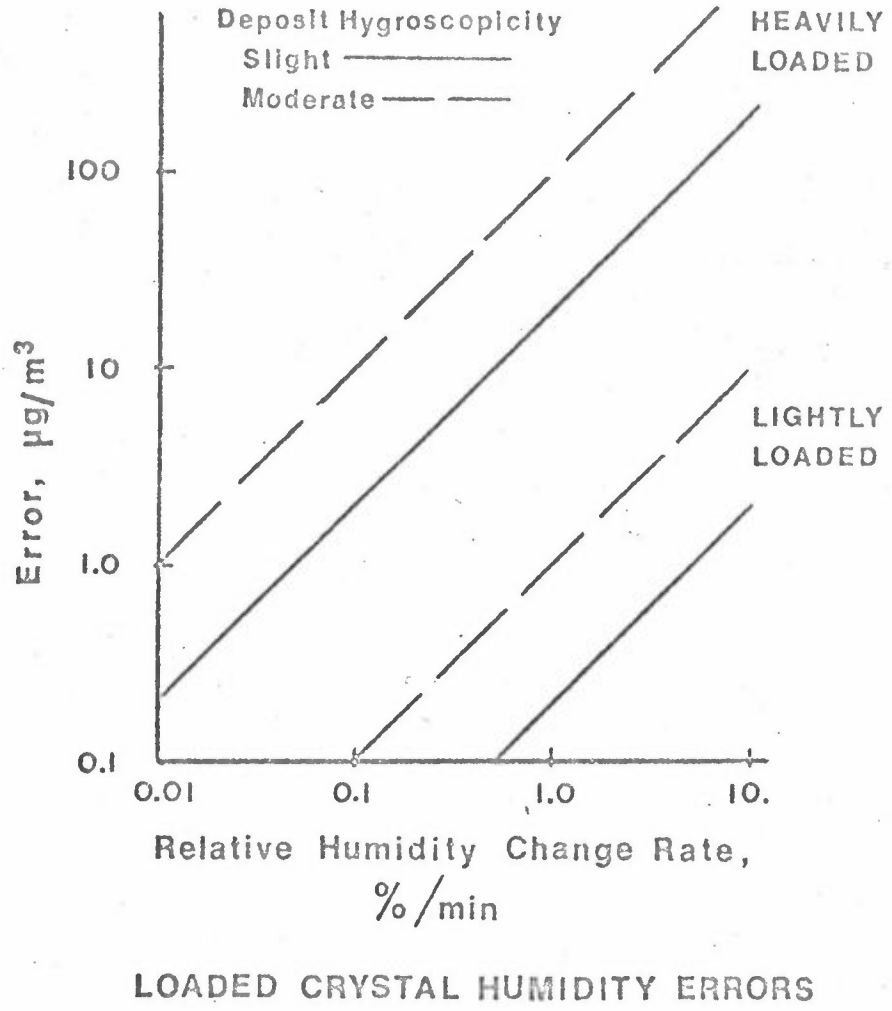

Figure 5-4. Errors Resulting from Inlet Air Relative Humidity Changes as They Affect the Mass of the Deposit Previously Collected on the Crystal Surface. (After Reference 6)

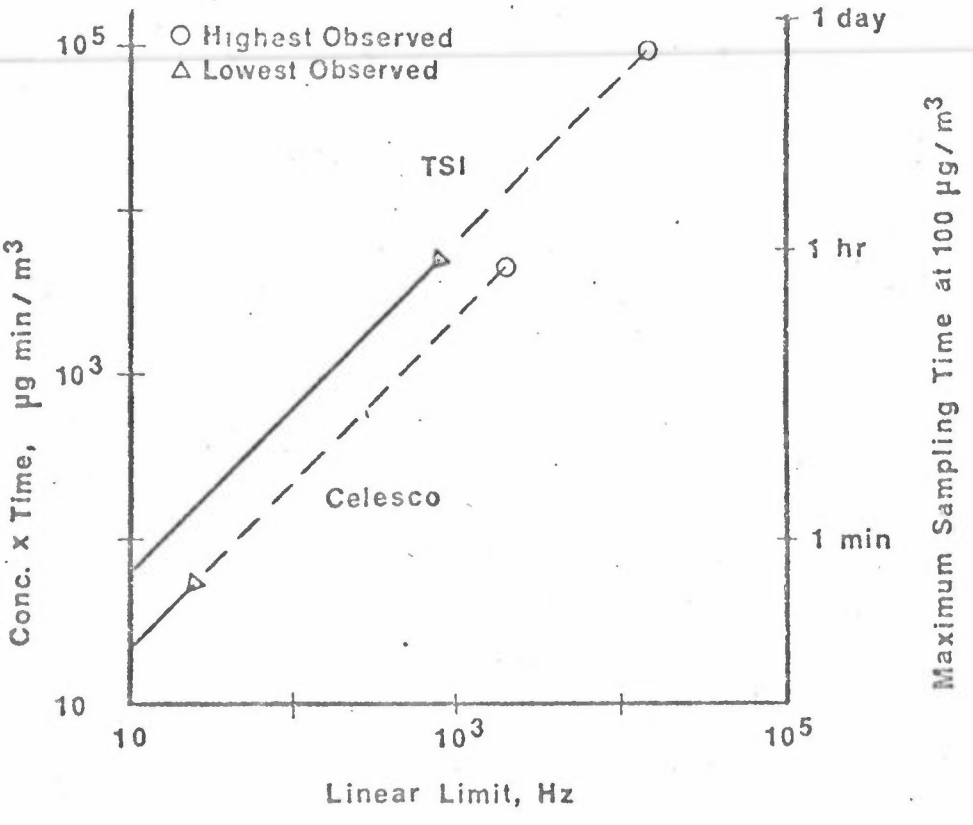

RANGES OF OBSERVED LINEAR RESPONSE LIMITS

Figure 5-5. Ranges of Observed Linear Response Limits and Corresponding Sampling Time, Concentration Products. (After Reference 6)

periods in hot, humid, unstable atmospheres. For many combinations of loadings and humidity change rates the signal noise may be become intolerable. The noise band width is twice the ordinate of Figure 5-4. This problem was clearly observable when relative humidity and concentration vs. time recordings were made in parallel. Since this error increases with relative humidity, heating the inlet air stream should reduce it. However, this test was not made.

Schulte (5) conducted tests to determine the interference due to humidity. He found that the humidity response was almost an order of magnitude greater than that for sulfur dioxide. This meant that if such a device was to be used for monitoring sulfur dioxide some method must be used to eliminate the effect of the water vapor. He considered three different methods for eliminating the water vapor before it reached the detector : 1) permeable membranes, 2) trapping and 3) separation. Results of work by others indicated that the first two methods would not be satisfactory so he tried the third method and obtained disappointing results. Gas chromatograph columns packed with 1) Chromosorb W and coated with polyphenyl ether, 2) silica gel and 3) alumina, were tried but none of them provided the needed separation.

In summary, two types of relative humidity induced errors have been observed, those associated with the crystal and its electrode and those stemming from the hygroscopic nature of the aerosol deposit. The former is significant only for the case of particle deposition by electrostatic precipitation while the latter is fundamental to the piezoelectric method and may lead to large errors under sampling conditions that involve wide variations in relative humidity. At present there does not seem to be any feasible method for isolating and eliminating the effect due to water humidity. It seems, however, that heating the air sample may reduce one or both of these basic problems.

Pressure

The frequency effects of gas pressure on quartz crystal microbalances have been studied by Stockbridge (9). In the study, Stockbridge concluded the following :

1) The frequency increased linearly with the pressure due to the effect of hydrostatic pressure on the elastic moduli of quartz.

2) The frequency decreased and the resistance increased linearly with $p^{\frac{1}{2}}$ due to the complex shear impedance of the gas, regarded as a viscoelastic fluid.

3) The frequency decreased with p due to sorption of gas molecules.

The frequency change due to the first two effects was dominant over that produced by gas sorption. Analysis showed that the gases adsorbed less than one monolayer on the crystal surface. The effect of mechnical hydrostatic pressure on the resonant frequency is given by the following equation :

$$\frac{1}{f_o}\frac{df}{dp} \simeq 15 \times 10^{-10}/\text{torr}$$

where

f_o is the resonant frequency, MHz
df is change in frequency due to dp
dp is the change in atmospheric pressure, torr

This error is small for normal atmospheric pressures and pressure fluctuations. A 10% change in atmospheric pressure would represent an error of about 0.05 $\mu g/M^3$

Particle Collection

The crystals in the Celesco unit are coated to assure collection of rigid particles. Celesco normally supplies their crystals coated with a proprietary material. In their study Daley & Lundgren (6) used coating of Dow-Corning 200 Fluid viscosity 10^5 cp. The coatings were applied using cotton swabs and spread as uniformly as possible. The coating thickness, as determined by the frequency change of approximately 7 kHz, was approximately 0.3 µm. Thicker coatings would probably be desirable, but it was found that they damped out the crystal oscillation. When collecting viscose particles, such as uranine at high relative humidities, no coating material was necessary.

The 50% cut size for the Celesco impaction jet was calculated to be 0.55 µm for unit density spheres. Sampling aerosols of 0.41 µm and 0.65 µm diameter polystyrene spheres confirmed this calculation, the former being sampled with a very low efficiency and the latter very high.

Two aspects of the TSI collection system were studied: the efficiency of the electrostatic precipitator and the distribution of the deposit on the surface. The former was determined by collecting a Collison generated 0.2 µm methylene blue aerosol doped with 10% uranine. The amount of uranine collected in various parts of the instrument was determined by fluorescence techniques (10). The size and position of the deposit was determined by microscopic observation.

The results of the uranine tracer study are summarized in Table 5-1. At least 20% of the sampled aerosol was collected in the inlet passage prior to the test crystal. This deposition can be attributed to the high electrid field in the vicinity of the electrode shaft which has a potential of 5000 v. Calculation of the field strength necessary to deposit 0.2 µm particles in the annular region surrounding the

electrode shaft, assuming a Boltzman charge distribution, confirmed that this probably was the cause. The 9.2% of the aerosol that went unaccounted for was probably collected on the down stream side of the crystal but was so thinly dispersed that recovery was not possible.

As shown in Table 5-1 70.4% of the entering aerosol was actually collected on the crystal surface. This figure is not a true measure of the fraction of the material actually sensed by the crystal, however, as som material was undoubtedly collected on inactive portions outside the electrode. This error is estimated to be less than 2% of the total aerosol entering.

It was found that the diameter of the TSI deposit was a function of the particle size involved, being ≈ 5.3 mm diameter for 0.2 μm diameter particles and decreasing to ≈ 2 mm for 20 μm particles. This is probably due to the increased ease of charging of large particles. As shown by the mass sensitivity distribution sketched in Figure 5-6, the differential mass sensitivity is highest near the crystal center. This result was subjectively confirmed for polydisperse aerosols by microscopic observations; a concentration of larger particles near the center was clearly observable.

Linear Response

The shapes of various particle deposition curves observed during Daley and Lundgren study (6) are sketched in Figure 5-7. Examples of the materials exhibiting each curve are given in the accompanying table. The curve shape predicted by simple analysis is represented by curve 1. In this case, as the deposit thickness increases, viscous and frictional losses also increase until additional deposit mass no longer vibrates with the crystal and therefore produces no frequency change. Because several additional factors, such as the distribution of the particles on the surface and

Table 5-1

Particle Collection in TSI Mass Monitor*
(After Reference 6)

Location	% Collected
Parallel Filter	100.0
Crystals	70.4 (σ = 2.6)
Precipitator Electrode	7.8
Electrode Chamber	7.4
Inlet Washings	5.2
Down Stream Filter and Washings	0.0
Unaccounted	9.2

*Average of 5 runs using uranine tagged 0.2 μm mmd methylene blue aerosol.

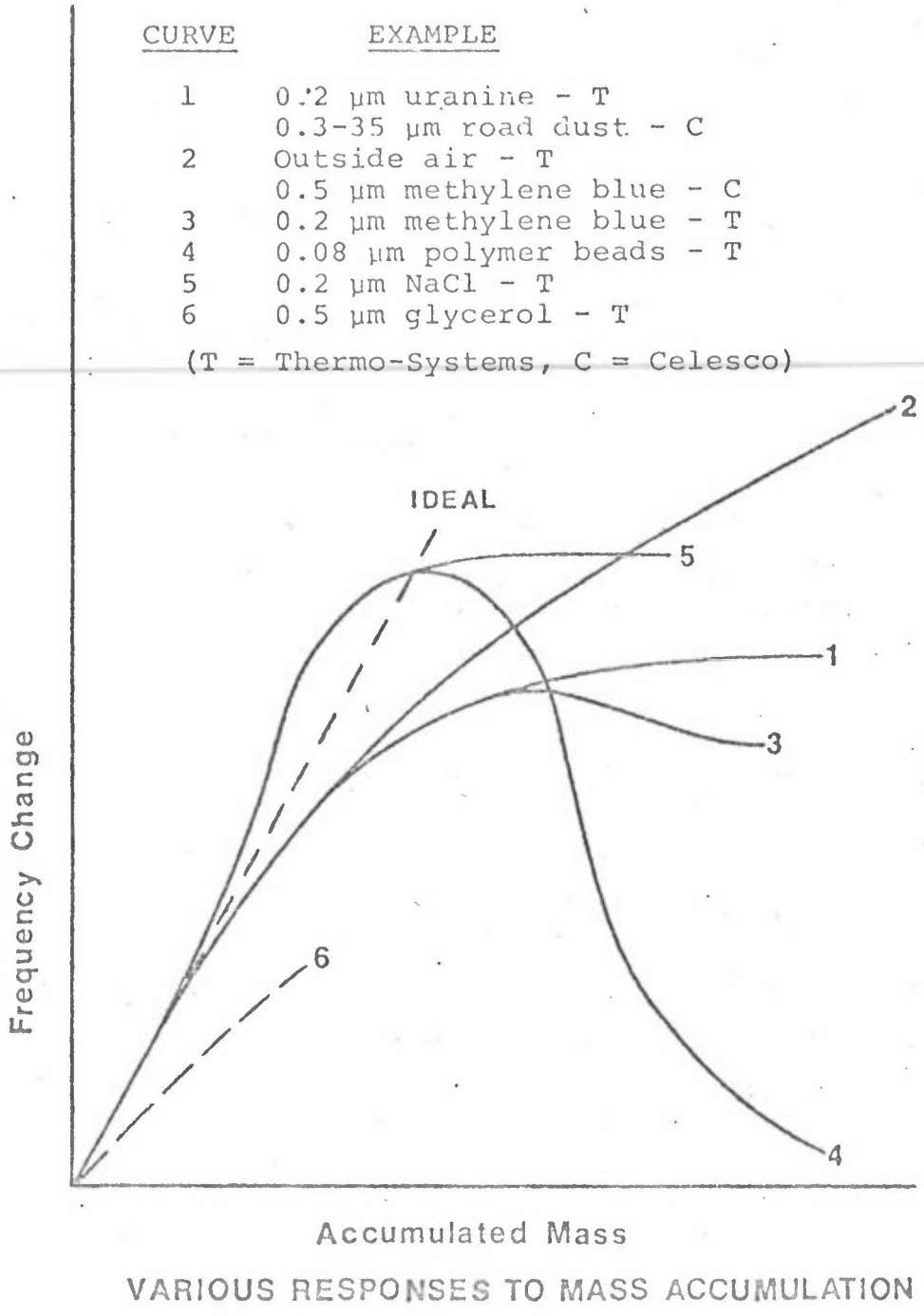

Figure 5-7. General Shapes of Mass Accumulation Curves Observed During Study with Examples for Each. (After Reference 6)

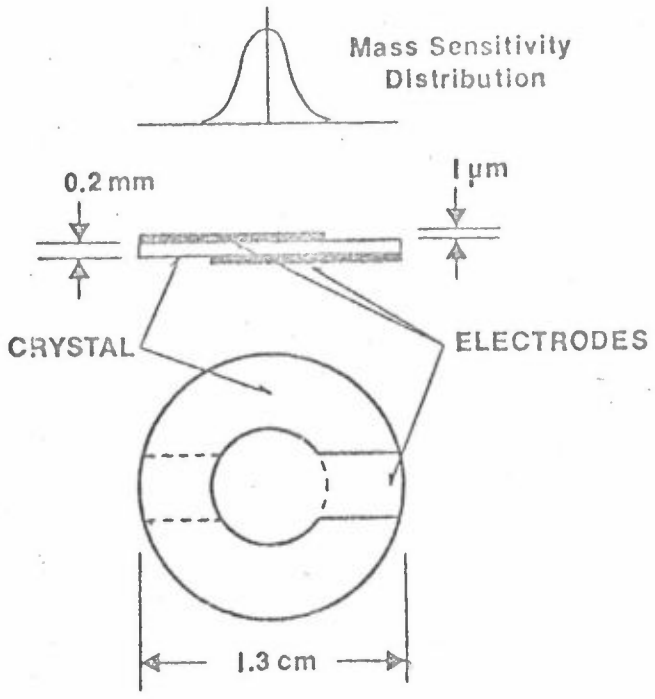

Figure 5-6. Sketch of Typical Crystal Showing Approximate Mass Sensitivity Distribution (After Reference 6)

agglomeration, influenced the process,: many other curve shapes were observed.

For the case of particle deposition by impaction, curve 2 is typical. The curve is characterized by a gradual decrease in slope and a second, approximately linear region. For particle collection by electrostatic precipitation a much wider variation in curve shape occurred. The decrease observed in curve 3 apparently resulted from agglomeration of small particles on the crystal surface. The larger particles formed by this process were not effectively sensed by the crystal (as discussed in the following section). Curve 4 is an extreme case of this phenomenon. Here essentially the entire deposit became agglomerated and the crystal returned to its original frequency. This process could be followed by microscopic observation at various stages. Agglomeration was most serious for small (≈0.1 μm) polymer spheres but there was evidence that it occurred in deposits of ambient aerosols as well.

The increasing slopes shown in curves 4 and 5 were apparently caused by preferable deposition in the less sensitive peripheral region in the initial period followed by a gradual shift to deposition in the more sensitive center. The shift probably resulted from changes in the electric field due to the initial annular deposit. For larger particles, curve 5, saturation was reached rather abruptly when the center became coated and no further change took place. For smaller particles, curve 4, agglomeration, already in progress, became more and more pronounced as the deposit thickened.

For aerosols of volatile compounds, there was considerable loss of material due primarily to volitilization under the corona. This was easily observed by simply changing to clean air and noting the immediate and steady decrease in frequency. One must conclude from this that the observed mass response for these volatile materials is less than expected. This case is shown by curve 6.

Figure 5-5 shows the relationship between the linear limit and the concentration time product. The importance of knowing the linear limit for any aerosol being sampled is apparent as some materials show non-linearity almost from the onset of sampling. For monitoring unknown aerosols, as would be the case in ambient conditions, it is impossible to know the linear limit. This means that a conservatively low value would have to be selected. From Figure 5-5 it can be seen that only relatively short continuous sampling periods would be possible.

A comparison of the data for uranine shown in Tables 5-2 and 5-3 show how increasing the relative humidity can dramatically increase the linear limit of a hygroscopic aerosol. Data in Tables 5-3 and 5-4 indicate that particle size is also important, the number of theoretically complete monolayers at the linear limit decreasing as particle size increases.

Mass Sensivity

Daley and Lundgren (6) determined the value of the mass sensitivity by various techniques, depending on the nature of the particles deposited. Uranine fluorescence, direct gravimetric determination, and parallel gravimetric filtration techniques were used for small particles. For particles large enough and uniform enough to be counted and sized with the light microscope, this technique was used. In all cases the deposition process was followed carefully to assure that the linear limit had not been exceeded. The Thermo-Systems unit was used as a basis for the calibration of the Celesco unit in the particle size range applicable to both. Results of the mass response studies are shown in Figure 5-8 and Table 5-5.

The expected values of the mass sensitivity were calculated from the experimentally determined relative mass sensitivity distributions, determined by traversing the crystal with an

Table 5-2

TSI Mass Monitor, Polydisperse Aerosol Response Summary (After Ref. 6)

Material	*Particle Size, μm	Deposit Diameter, mm	Crystal Sensitivity, Hz/μg	Linear Response Limit			Saturation	
				kHz	μg	$\frac{\mu g}{mm^2}$	kHz	$\frac{\mu g}{mm^2}$
Ariz. road dust	0.3-35	3.8	255	≈0.5	≈2.5	≈0.2	0.8	0.7
Methylene blue-uranine, 9:1, 22% RH, 1.5 mg/m^3	0.2	5.3	190	0.7	3.5	0.16	2.0	0.5
Ariz. road dust 27% RH	0.3-3	4.3	230	0.7	2.7	0.21	>3.0	>1.
$(NH_4)_2SO_4$, 27% RH	0.2	5.0	205	0.9	4.5	0.23	1.1	0.3
Laboratory air, ≈50% RH	-	5.	205	1.0	5.0	0.25	3.5	0.4
NaCl, 27% RH, 1.5 mg/m^3	0.2	4.3	230	1.0	4.5	0.30	3.5	0.9
Uranine, 45% RH	0.5	5.3	190	1.5	7.5	0.35	-	-
$CaSO_4 \cdot 1/2\ H_2O$, ≈50% RH	1-3	5.	205	1.5	7.2	0.5	2.5	1.3
Outside air, high visibility, 60% RH	-	5.	205	1.5	7.2	0.5	>4.	>1.5
Glycerol	0.5	6.4	155	3.5	23.	0.70	9.5	3.5
Dimethyl polysiloxane, viscosity = 10^5 cp	0.5	6.4	155	4.1	27.	0.83	9.5	4.
Methylene blue-uranine, 9:1, 22% RH, 0.2 mg/m^3	0.2	5.3	190	4.0	21.	0.97	20.	>>3.
NaCl, 27% RH, 0.15 mg/m^3	0.2	4.3	230	4.0	17.	1.5	4.3	1.6
Dimethyl polysiloxane viscosity = 10^5 cp	0.2	6.4	155	9.0	60.	1.8	9.5	2.0
Uranine, 75% RH	0.5	5.3	190	12.0	63.	3.0	>15.	>4.2

*Ranges estimated optically; 0.2, 0.5 μm aerosols were Collison generated, see text.

Table 5-3

Celesco Quartz Crystal Microbalance Aerosol Response Summary (After Ref. 6)

Monodisperse Materials	Particle size, μm	Linear Response Limit				Saturation	
		Hz	μg	μg/mm²	mono-layers	Hz	μg/mm²
Polystyrene beads	0.41	Not Collected					
Polystyrene beads	0.65	120	0.043	3.5	10.	215	9
Polystyrene beads	0.83	75	0.024	2.2	4.7	275	20
Polystyrene beads	1.24	25	0.009	1.0	1.1	>60	>10
Polyvinyl toluene beads	1.89	30	0.011	1.6	1.3	>300	>20
Polydisperse Materials							
Methylene blue-uranine, 9:1, 27% RH	0.5	75	0.027	2.3	N.A.	>600	>30
Arizona road dust	0.3-35	-	-	-	N.A.	150	≈20
Uranine, 27% RH	0.5	100	0.036	3.0	N.A.	>400	>70
Uranine, 60% RH (Crystal not coated)	0.5	1900	0.68	56.	N.A.	>2000	>100

NOTE: Crystal sensitivity of 2800 Hz/μg used in calculation of this table. Deposit diameter of 0.4 mm for all materials except 1.24 and 1.89 μ beads which had 0.35 and 0.3 mm deposits, respectively.

Table 5-4

TSI Mass Monitor, Monodisperse Aerosol Resononse Summary (After Ref. 6)

Material	Particle Diameter, μm	Deposit Diameter, mm	Crystal Sensitivity, Hz/μg	Linear Response Limit				Saturation	
				KHz	μg	$\frac{\mu g}{mm^2}$	Monolayers	KHz	$\frac{\mu g}{mm^2}$
Polystyrene	0.08	5.0	205	1.6	8.8	0.40	8.0	4.0	1.2
Polystyrene	0.14	4.3	230	1.9	7.5	0.57	7.7	5.4	2.5
Polystyrene	0.41	4.3+	230	3.7	1.45	1.15	4.0	4.2	1.3
Polystyrene	0.65	4.5	220	3.8	15.3	1.10	3.0	4.5	1.2
Polystyrene	1.24	4.0	240	6.0	25.	2.0	2.6	17.	5.
Polyvinyl toluene	1.89	3.4	265	No data					
Styrene divinyl-benzene copolymer	7.8*	2.5	285	Not detected efficiently					
Paper mulberry pollen	12.	1.5	300	Not detected efficiently					
Ragweed pollen	20.	1.5	300	Not detected efficiently					
Glass beads	34.	Not collected							

*Approximately normally distributed with mass mean diameter of 7.8 μ and standard deviation of 1 μ.
+Not measured but determined from plot of particle diameter vs. deposit diameter for other sizes.

Table 5-5

Experimental Crystal Mass Sensitivity Determinations
(After Reference 6)

Test Aerosol and Technique	Runs	Sensitivity, Hz/μg Observed†	Expected	Sensing Eff., %
Thermo-Systems Unit				
Methylene blue-uranine, 0.2 μm mmd.				
Uranine fluorescence	5	273 ± 16	192	142
Parallel filtration	2	268	192	138
Direct gravimetric	4	198 ± 22	192	103
1.89 μm polymer beads				
Particle count	1	280	265	105
Arizona Road dust, ≈2.5 μm mmd				
Direct gravimetric	5	174 ± 26	192	91
7.8 μm polymer beads				
Particle count	1	107	285	37
12 μm pollen				
Particle count	1	30	300	10
Particle count*	1	33	105	32
20 μm pollen				
Particle count	3	≈0	300	≈0
Particle count*	1	≈0	105	≈0
34 μm glass beads	1	Not Collected		
Celesco Unit				
Uranine, 0.5 μm mmd				
Fluorescence	4	3075 ± 1140	2830	108
0.65 μm polymer beads				
Thermo-Systems P.M.M.	3	2950 ± 1200	2740	107
1.24 μm polymer beads				
Thermo-Systems P.M.M.	3	3500 ± 1600	2830	123
1.89 μm polymer beads				
Particle count	1	4200	4800	87
12 μm pollen				
Particle count	1	≈0	2830	≈0

*Coated crystal with particle application by settling.
†Limits represent 2 standard deviations of variance among runs.

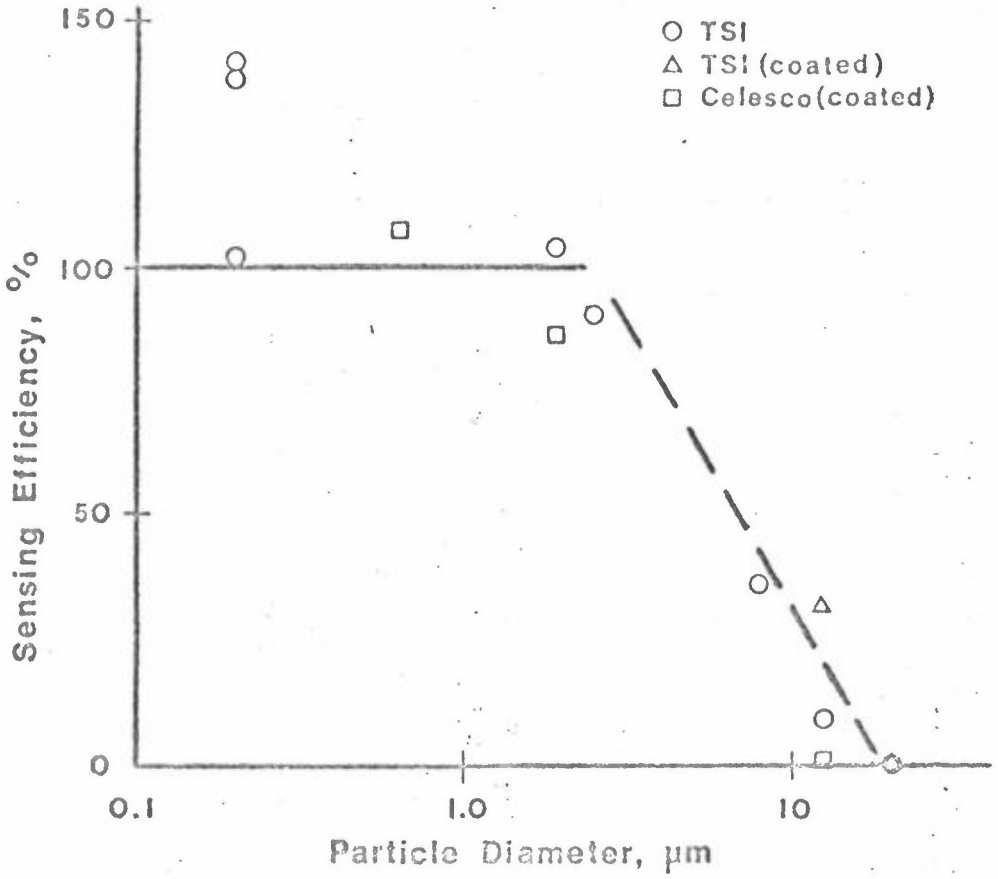

Figure 5-8. Ability of Crystals to Sense Particles of Various Sizes. (After Reference 6)

impaction jet of approximately 0.5 mm diameter, and using the theoretical equation. In neither instrument was the deposit area conterminous with either the electrode area or the active area. In the case of the Celesco crystals the mass sensitivity varied much more than would be expected both within a single crystal and from crystal to crystal, the ratio of the maximum to average sensitivities in the electroded region ranging from 4:1 to 8:1. A value of approximately 2.5:1 would be expected for crystals with the electrode area conterminous with the active area (11). Unfortunately, the maximum sensitivity did not always occur at the crystal center with the result that the impactor deposit often fell in a region of rapidly changing sensitivity. This accounts for the large variance of the mass sensitivity data for the Celesco unit since even a small error in position led to a large change in sensitivity.

For the TSI crystals, the mass sensitivity distribution showed significant activity beyond the electrode perimeter indicating that trapping was not complete. The effect of this was to reduce the averate sensitivity over the entire electrode from 180 to 160 Hz/µg. The reduction, however, was more than compensated for by the fact that particles were not collected on the lower sensitivity perifery of the electrode. The mass sensitivities for various size deposits are found in Tables 5-2, 5-4 and 5-5. A reasonable average value for the mass sensitivity of the TSI unit is 200 Hz/µg. This value should normally be in error by no more than ±15%.

The results for particle sizes less than 1.5 µm generally support the mass sensitivity prediction techniques used, the average error being ± 15%. The data indicate a decrease in sensing efficiency beginning at about 2 µm for spherical particles. This trend is shown graphically in Figure 5-8. There seems to be little difference between the data from the coated 10 MHz crystals used in the Celesco device and the uncoated 5 MHz crystals used in the TSI Mass Monitor.

It is possible that the coating compensates for the increased frequency (and therefore increased dislodging forces) in the former case. The difference between the Celesco and TSI units for 1.89 μm spheres is probably due to experimental errors, the most significant being the crystal position in the Celesco unit. For 12 μm particles on 5 MHz crystals there was a four fold increase in the sensing efficiency when a coating was used.

REFERENCES

1. Carpenter, T. E., "The Design, Construction, and Calibration of a Piezoelectric Cascade Impactor for Monitoring Aerosols," M.S. Thesis (Civil Engineering), Purdue University, Lafayette, Indiana, 1972.

2. Carpenter, T. E., and D. L. Brenchley, "A Piezoelectric Impactor for Aerosol Monitoring," Am. Ind. Hyg. Assoc.J., 33:503-510 (1972.

3) Herling, Robert, W. Karches and J. Wagman. "A Comparison of Automotive Particle Mass Emissions Measurement Techniques," Central States Meeting of the Combustion Institute, Univ. of Mich., Ann Arbor, Mich., March 23-29, 1971.

4. Imada, I., and P. K. Mueller, "Evaluation of a Piezoelectric Quartz Crystal Microbalance for the Continuous Measurement of Aerosol," AIHL Report No. 114, Air and Industrial Hygiene Laboratory, State of Calif. Dept. of Public Health, Berkeley, Calif. (1971).

5. Schulte, H. F., "The Design, Construction and Evaluation of a Piezoelectric Sorption Detector for Sulfur Dioxide", M. S. Thesis (Civil Engineering), Purdue University, Lafayette, Indiana, 1973.

6. Daley, P. S. and D. A. Lundgren, "The Performance of Piezoelectric Crystal Sensors Used to Determine Aerosol Mass Concentrations," 1974 American Industrial Hygiene Conference, Miami, Florida, May 12-17, 1974.

7. Lundgren, D. A., and D. W. Cooper, "Effect of Relative Humidity on Light Scattering Methods of Measuring Particle Concentration, " J. Air Pollution Control Assoc. 19:243-247 (1969).

8. Junge, C. E., Air Chemistry and Radioactivity, p. 133, Academic Press, New York (1963).

9. Stockbridge, C. D., "Effects of Gas Pressure on Quartz Crystal Microbalances," Vac. Microbalance Techn., 2, 147 (1966).

10. G. K. Turner Associates, "The Determination of Fluorscein," Palo Alto, Calif. (1968).

11. Sauerbrey, G. Z., "Verwendung von Schwingquarzen zur Wagung Dunner Schichten und zur Microwagung," Zeits. Phys., 155:206-222 (1959).

Chapter 6

USE OF THE PMM

This report gives the results of the design and construction phases for the NILU PMM. However the instrument can not be used until it has undergone extensive laboratory and field tests. The purpose of this chapter is to outline how these tests might be carried out. Since the design and conduct of this test program is the responsibility of NILU, these are only suggestions. As indicated in Chapter 5 there are a number of limitations and sources of error. If these are not properly corrected or evaluated the PMM data will be useless. The work of Daley and Lundgren (1) must there be considered in conducting these tests.

Additions and Alterations

All of the components on the instrument are operational. However there are a number of things which should be altered on this prototype instrument. Some of them we know about and they are listed below. Others we don't know about but they will become apparent in the course of the laboratory and field tests.

-- Install a microswitch inside the chassis to automatically turn off the EP when the oscillator clip containing the crystals is removed from the instrument. When doing this be sure that the switch lever doesn't short out on the male pins or the chassis.

-- A sample pretreatment and flow control system must be added. If the inlet sample flow is heated this will reduce the interference caused by relative humidity. Once this system has been built, it must be tested to determine the amount of sample loss and any changes in aerosol properties.

-- The oscillator clip should be fastened to the Teflon sampling head. This should be done to eliminate leaks but at the same time allow easy removal of the clip.

-- The EP adjustment screw and wire clip is too crude. It should be redesigned.

-- The sample flow to the collecting electrode may have to be changed. Now the sample enters the Teflon sampling head and it must make a 90 degree change in direction before it passes around the discharge electrode (needle) of the EP. If sample loss is a problem here then the design must be changed.

Laboratory Tests

There are a number of laboratory tests which must be performed:

-- Determine the sample losses in the instrument.

-- Determine the performance of the electrostatic precipitator. Determine the adjustments and sample flow rate for best operation.

-- Determine the collection efficiency of the EP.

-- Determine the instrument response to fluctuations in temperature and relative humidity.

-- Check the linearity of the instrument response and determine the mass sensitivity.

Uranine dye may be used to help determine wall losses and the efficiency of the electrostatic precipitator. This dye is put into water and then used in an aerosol enerator (2,3,4). If a metallic aerosol can be used then similar tests can be performed using X-ray fluorescence spectrometry (5). Dr. Stiles has agreed to perform these analyses and he has already sent one shipment of Fluoropore (Teflon) filters and holders to do this type of work. In addition Dr. Stiles can also use beta gauging techniques on these filters to determine total mass of the sample.

Field Tests

Preliminary tests should be performed with the instrument in the aircraft. This will allow testing of the instrument in conjunction with the sample flow control and pretreatment systems. The data from the PMM should be compared with that obtained by conventional filtration techniques. This would be achieved by using the existing filter system on NILU's aircraft. The Fluoropore filter and holder provided by Dr. Stiles could also be used here. This technique has the advantage that it could provide both mass measurements and elemental analyses. Such analyses would definitely be of interest in the Long Range Transport research work.

References

1. Daley, Peter S. and Lundgren, Dale A.
The Performance of Piezoelectric Crystal Sensors Used to Determine Aerosol Mass Concentrations
American Industrial Hygiene Conference
Miami, Florida 12-17 May 1974

2. Carpenter, T. E.
The Design, Construction and Calibration of a Piezoelectric-Cascade Impactor for Monitoring Aerosols
M. S. Thesis, School of Civil Engineering
Purdue University 1972
West Lafayette, Indiana

3. Schulz, E. J., Duffee, R. A., Mitchell, R. I. and Ungar, E. W.
A Tracer Technique to Measure Deposition of Stack Emissions
Industrial Hygiene Journal, P. 343 (1960)

4. Dumbauld, R. K.
Meteorological Tracer Technique for Atmospheric Diffusion Studies
Journal of Applied Meteorology, 1:4, p 437 (Dec. 1962)

5. Dzubay, T. G. and R. K. Stevens
Applications of X-ray Fluorescence to Particulate Measurements
Second Joint Conference on Sensing of Environmental Pollutants--- Instrument Society of America
Washington, D. C. December 10-12, 1973